# NORTHERN CALIFORNIA GEOLOGICAL SOCIETY

c/o CALIFORNIA DIVISION OF MINES AND GEOLOGY
FERRY BUILDING SAN FRANCISCO, CALIFORNIA 94111

April Meeting - Wednesday, April 17, 1974

OPHIOLITES, by Robert G. Coleman, U.S. Geological Survey

Leopard Cafe, 140 Front Street, San Francisco
Social Hour: 11:30 A.M.; Luncheon: 12:00 Noon

Reservations: Please make your reservations by Tuesday, April 16.

USGS and Stanford call Vern Stephens - 323-811, Ext. 2717

Socal 320 Market call Ginger Meese - 894-0270

Socal 555 Market call Judy Bonilla - 894-5352

Others - call Ginger Meese or Tom Wright - 894-0725

FIELD TRIP: Ophiolites in the Mesozoic Subduction Zone of Central California, Mr. R. G. Coleman, leader.
Saturday, April 20th (9:00 a.m.-6:00 p.m. approximately)

A bus trip to the Red Mountain area of the southern Diablo Range, where Franciscan rocks and the Great Valley Sequence crop out adjacent to the Coast Range Thrust Fault. We will walk through a complete, classic section of oceanic crust. (Boots or heavy shoes recommended). Picnic lunch in a pleasant rural setting.

Bus pick-up in San Francisco (± 8:30 a.m.), San Mateo (± 9:00 a.m.), and Dublin (± 9:40 a.m.). Bring a lunch; cold beverages provided.

Cost (bus, guidebook and beverages): about $8.00 (may be adjusted slightly).

For reservations (and further details) send your check ($8.00 each) to:
Mr. T. L. Wright, P. O. Box 3069, San Francisco, CA 94119 (phone 894-0725)

Earl Hart

FIELD TRIP: Ophiolites in the Mesozoic Subduction Zone of Central California

Leader: Dr. Robert G. Coleman, U.S.G.S. (assisted by Charles C. Bishop, California Division of Mines and Geology)

Saturday, April 20th, 1974

Schedule:

Bus pick-ups: (X)

San Francisco/Marin - 8:00 a.m.
In front of Marina Safeway, Marina Blvd. at Buchanan. Park in public lot across the street.

Peninsula - 8:30 a.m.
Foster City, Hillsdale and Shell Blvd., in front of Wells Fargo Bank Building.

East Bay - 9:15 a.m.
Dublin, shopping center, between Rhodes and Holiday Inn.

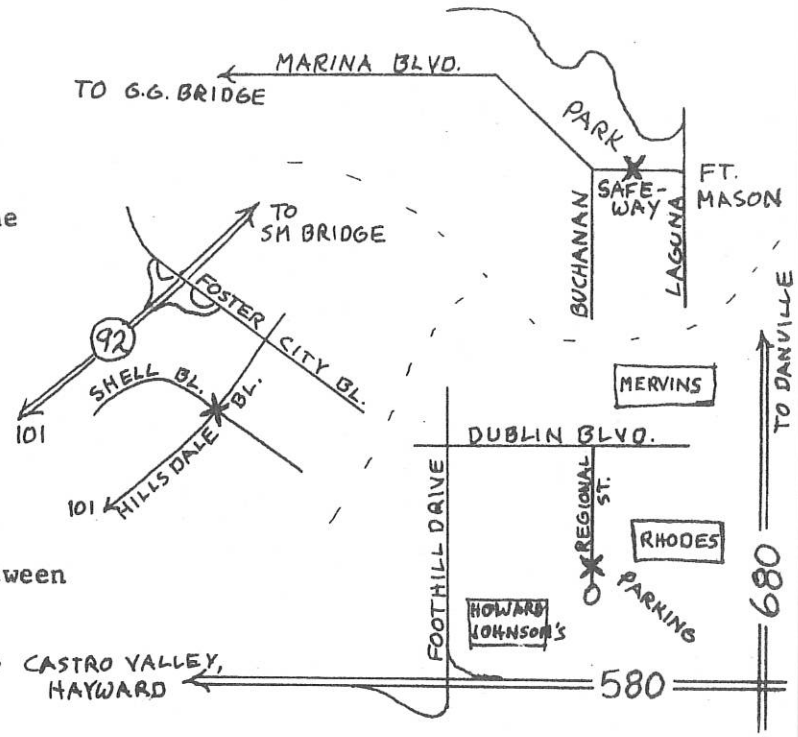


Itinerary: East on 580 to Livermore; east through Corral Hollow to 580/5; south to Del Puerto Canyon Road (near Patterson); west into outcrop.

Return (times approximate): Dublin - 5:45; Foster City - 6:15; S. F. - 6:45 p.m.

Bring a lunch. Beer and soft drinks will be provided. Wear boots or heavy shoes - there will be some walking. (Hill-climbing is optional!)

References:


Maddock, M.E., Mt. Boardman Quad, Calif. DMG MS-3 (1964) Included with Guidebook

Geologic Map of Calif. (DMG) San Jose Sheet (for sale on trip- $1.58)
San Francisco Sheet

Huey, A. S., Geology of the Tesla Quadrangle, DMG Bull. 140 (1948) (out-of-pr.)

Bailey, Blake and Jones, On-Land Mesozoic Oceanic Crust in California Coast Ranges, USGS Prof. Paper 700-C, (1970), pp.C70 - C81

Bishop, C. C., Upper Cretaceous Stratigraphy on the West Side of the Northern San Joaquin Valley, DMG SR-104 (1970)

Coleman, R.G., Plate Tectonic Emplacement of Upper Mantle Peridotites Along Continental Edges, Jour. Geophys. Res., v. 76 (1971), pp. 1212-1222

Ernst, W.G., Tectonic contact between the Franciscan melange and the Great Valley sequence - crustal expression of a Late Mesozoic Benioff Zone, Jour. Geophys. Res., v. 75 (1970), pp. 886 - 902

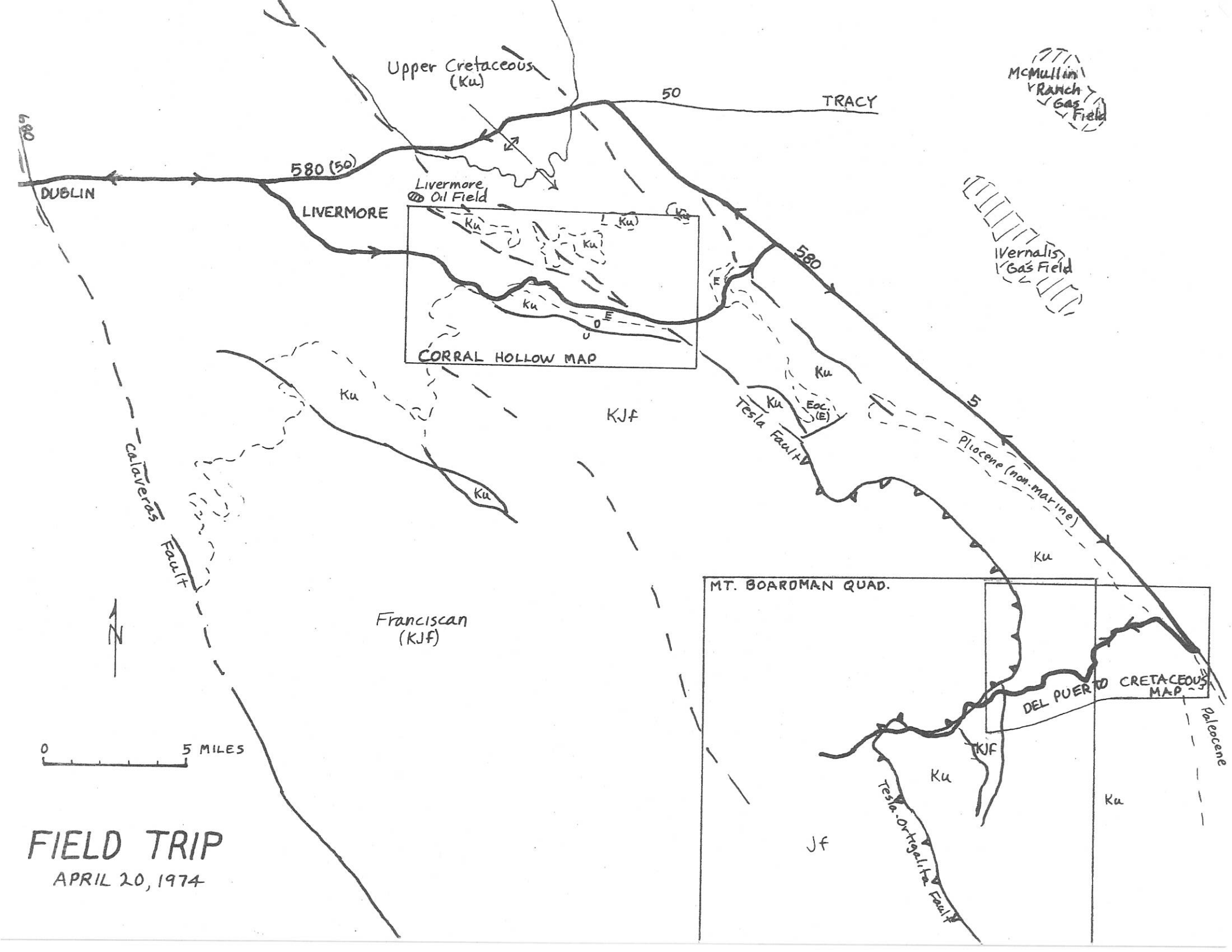
Upper Cretaceous (Ku)
50
TRACY
McMullin Ranch Gas Field
580
580 (50)
DUBLIN
LIVERMORE
Livermore Oil Field
Ku
CORRAL HOLLOW MAP
Vernalis Gas Field
580
5
KJf
Tesla Fault
Eoc (E)
Pliocene (non-marine)
Calaveras Fault
Franciscan (KJf)
MT. BOARDMAN QUAD.
DEL PUERTO CRETACEOUS MAP
Paleocene
Jf
Tesla-Ortigalita Fault
0 5 MILES
FIELD TRIP
APRIL 20, 1974

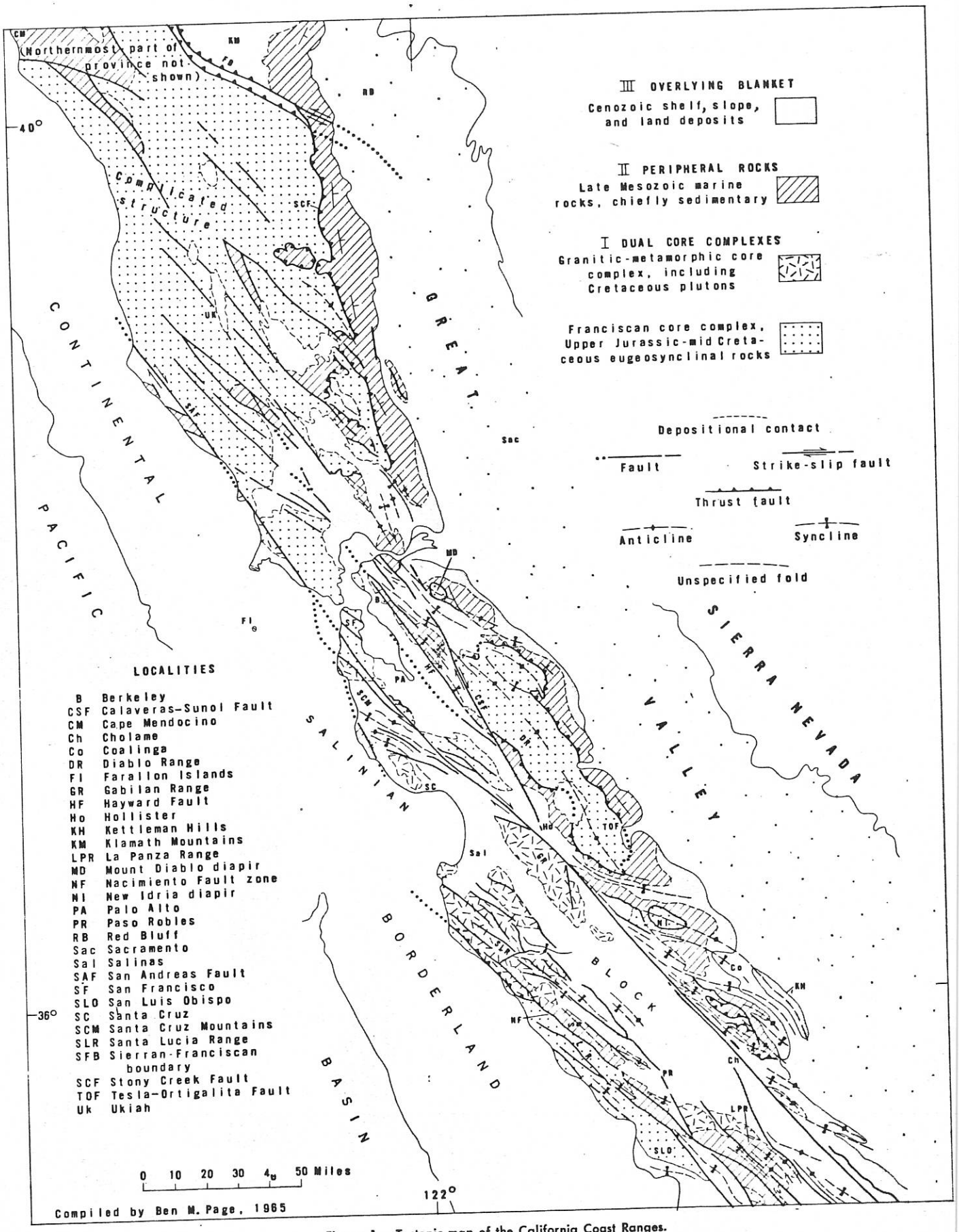


Figure 1. Tectonic map of the California Coast Ranges.

LIVERMORE OIL FIELD

(Abstract by Pat Fazio, McCulloch Oil Co., from Pacific Section AAPG, March, 1968)

The Livermore Field on the east edge of the Livermore Basin was discovered in January, 1967, by the McCulloch Oil Corporation at their Greenville Investment Group #1 well, which initially produced 567 b/d of 22° oil from the interval 1846-2024 feet. Two areas of production are established by four wells in the Main Area and by two wells in the East Area. Production is from Miocene, Eocene and possibly Cretaceous sands. The stratigraphy and structure is very complex and not yet clearly delineated. A total stratigraphic section exceeding 15,000 feet has been penetrated by wells in the field. Structure in the Main Area is basically a west plunging nose with separate reservoirs probably being formed by north trending faults. An alternative solution to explain the separate reservoirs is that rapid stratigraphic changes /discrete transgressive sands deposited up a pre-existing nose/ in the shallow water Cierbo formation (Miocene) over a structural nose form separate traps. Oil in the East Area appears to be trapped by the Carnegie Fault which has about 7000 feet of stratigraphic separation. The field appears to be of marginal economic significance (480 b/d at present) but is important because it opens a new oil province.

- - - - -

Data from Division of Oil and Gas, Oil and Gas Fields of Northern California (1973)

Deepest well: McCulloch (now Hershey) Nissen #3, spudded 9/67, T.D. 6819 feet in Moreno(?), Late Cretaceous

| Producing Zones: | Av. Depth | Av. Net Thick. | Age | Fm. | API Gr. |
|---|---|---|---|---|---|
| Greenville | 880 - 2000 ft. | 40 - 250 ft. | late Miocene | Cierbo | 25 - 29 |
| (unnamed)* | 5300 | 25 | Eocene | Tesla | 36 |

Production Data (Jan. 1, 1973)

65 acres proven 7 producing wells 121,434 bbls. oil, no gas, in 1972

90 acres maximum, 32 wells drilled, 10 completed

Cumulative production- 771,466 bbls. oil, no gas

Peak production- 161,829 bbls. in 1969

*One well only, abandoned in 1969

# LIVERMORE OIL FIELD

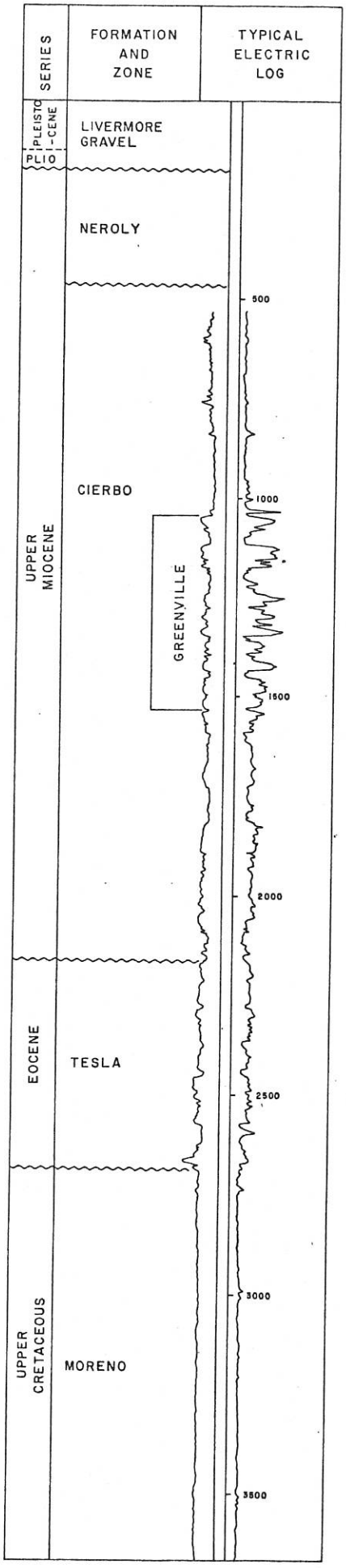


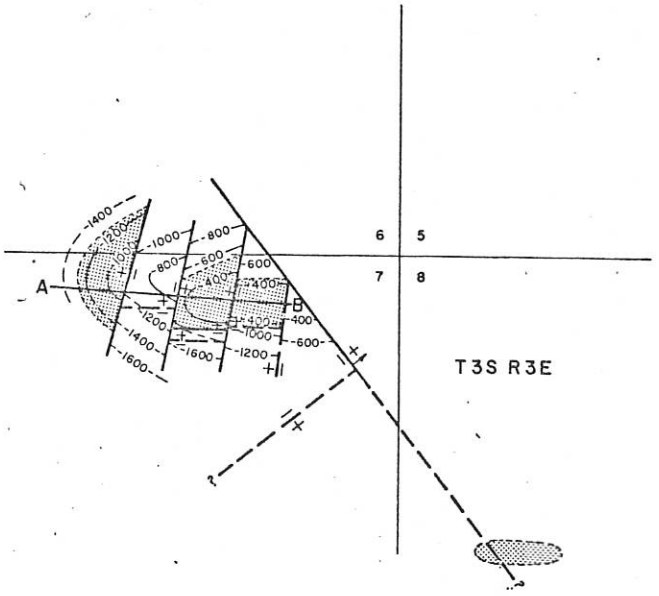


CONTOURS ON TOP OF GREENVILLE SANDS
SCALE 1" = 2000'

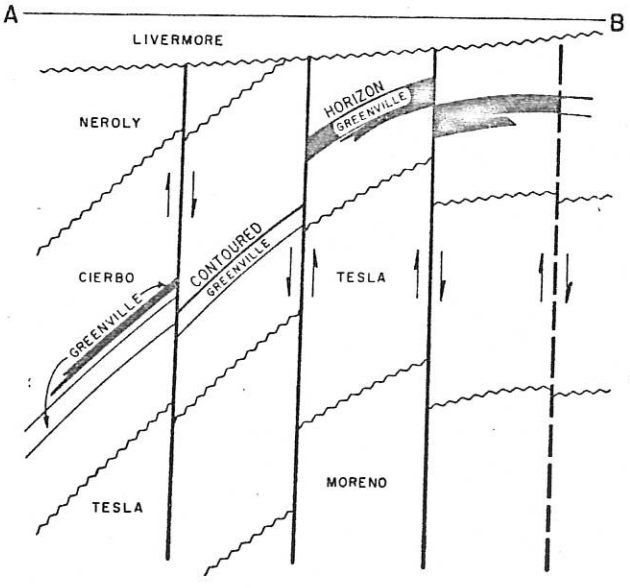

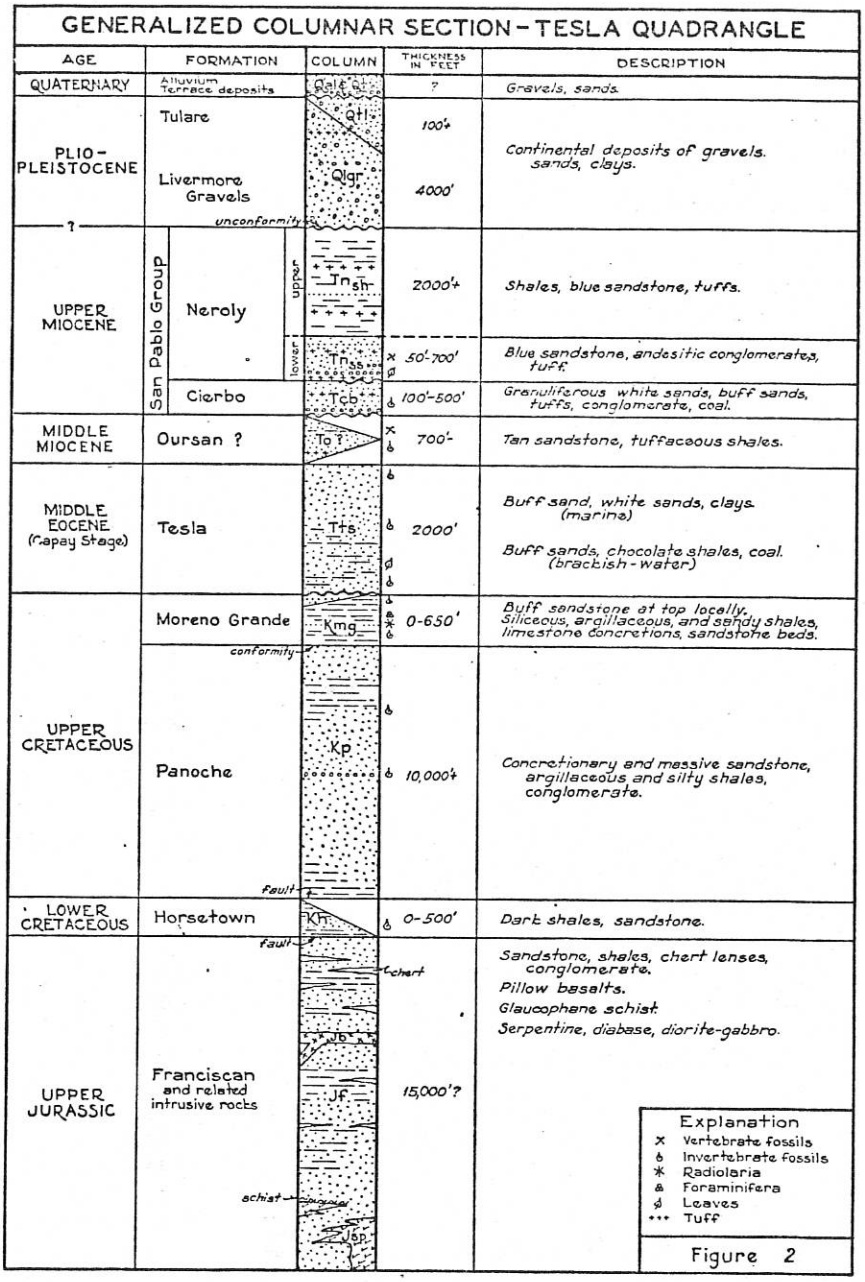


FIGURE 2. Generalized columnar section, Tesla quadrangle.

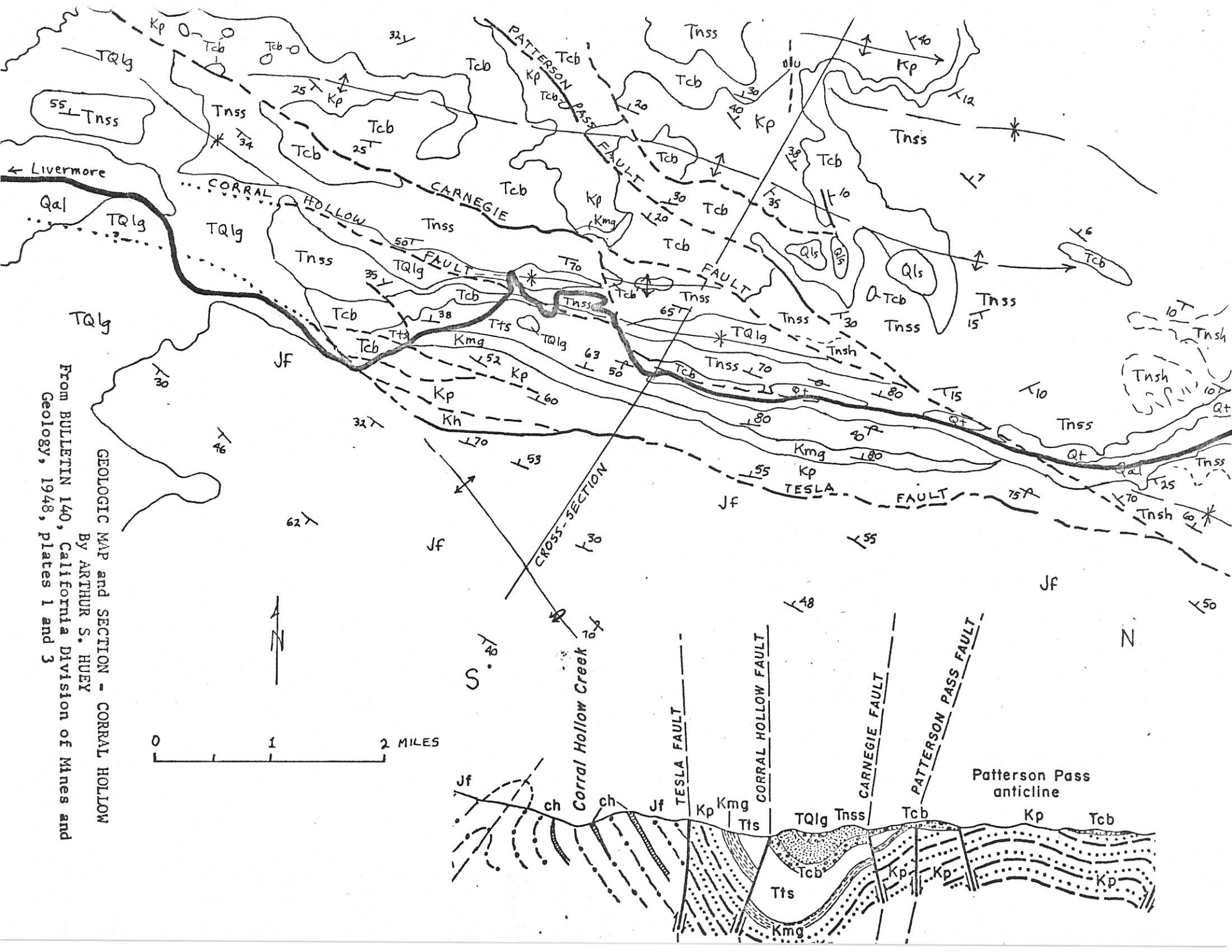


GEOLOGIC MAP and SECTION - CORRAL HOLLOW

By ARTHUR S. HUEY

From BULLETIN 140, California Division of Mines and Geology, 1948, plates 1 and 3

## ABSTRACT

Rocks of Late Cretaceous age crop out along the western side of the northern San Joaquin Valley. These rocks were first mapped and described by Anderson and Pack in 1915 and divided into the Panoche and Moreno Formations. Since then other workers have divided the rocks into groups, formations, and members.

A two-fold subdivision of the Panoche Formation can be recognized and mapped over a large part of the western side of the northern San Joaquin Valley. Further subdivision may be made locally, but rapid lateral lithologic variations and lack of diagnostic fossils make it difficult to recognize or map these smaller members for any appreciable distance.

Along Del Puerto Creek a section consisting of nearly 20,000 feet of marine Cretaceous rocks of the Panoche Formation is well exposed. These rocks are divided into seven units. The oldest is a dark greenish black shale ranging in age from the Lower Cretaceous Albian Stage to the Upper Cretaceous Turonian Stage. This unit is about 1500 feet thick and represents the lowermost of the two-fold subdivisions of the Panoche. It has been named the Adobe Flat Shale Member by Maddock (1964) and is correlative with the Pacheco Group of Taliaferro (1943, p. 131).

Units II through VII represent Taliaferro's Asuncion Group and are composed of light gray arkosic sandstones and medium brown siltstones and claystones and a lens of conglomerate. The sandstones and conglomerate were deposited by turbidity currents below wave base. Fossils present are characteristic of the Coniacian to Campanian Stages of the Upper Cretaceous. The upper gradational contact of unit VII with the overlying Moreno Formation marks the transition from a deep water to a shallow water environment.

The Moreno Formation is composed of brown clay shale and light gray sandstone. An upper sandy facies, the Garzas Member, can be recognized and mapped from Del Puerto Creek south to Garzas Creek. The Moreno, along the eastern flank of the Diablo Range, was deposited near shore in relatively shallow water. A land mass stood to the west and the deeper parts of the basins of deposition were to the east. Some of the sandstones of the Moreno Formation in the Del Puerto Creek area were deposited by turbidity currents. Foraminifera belonging to Goudkoff's D-1, D-2, and E zones occur in shales of the Moreno. Megafossils present are characteristic of the Campanian and Maestrichtian Stages of the Upper Cretaceous.

The biostratigraphic and lithologic equivalents of many of the subsurface units can be recognized in the surface exposures. The units encountered in the Shell Oil Company Elfers 36X-28 well can be correlated with a measured section of Upper Cretaceous rocks along Del Puerto Creek.

Three unconformities were recognized in the Upper Cretaceous sequence of this area. An understanding of these structural features helps explain some of the stratigraphic problems. Warping of the floor of the basin of deposition resulted in variations in the submarine topography. Because the sediments were deposited by turbidity currents, the topographically low areas were filled with coarse clastic material before the higher regions received any appreciable amount of sediment. Where these local structural irregularities can be recognized, it can be seen that some of the lateral facies changes are the result of local topographic relief.

The clastic material in most of the Panoche Formation was derived from a granitic and metamorphic terrain. The Campanian conglomerates in unit III contain Franciscan type rocks and were derived from a western land area. These conglomerates are younger than most of the conglomerates exposed to the south, particularly along Quinto Creek. Sandstones in units V, VI, and VII were deposited by turbidity currents moving in a northwest and southeast direction in the Del Puerto Creek area. Much of the sediment was derived from the west and much of this probably represents reworked Upper Cretaceous sedimentary rocks. The location of the source area of the granitic and metamorphic rocks could not be determined from the study of this limited area.

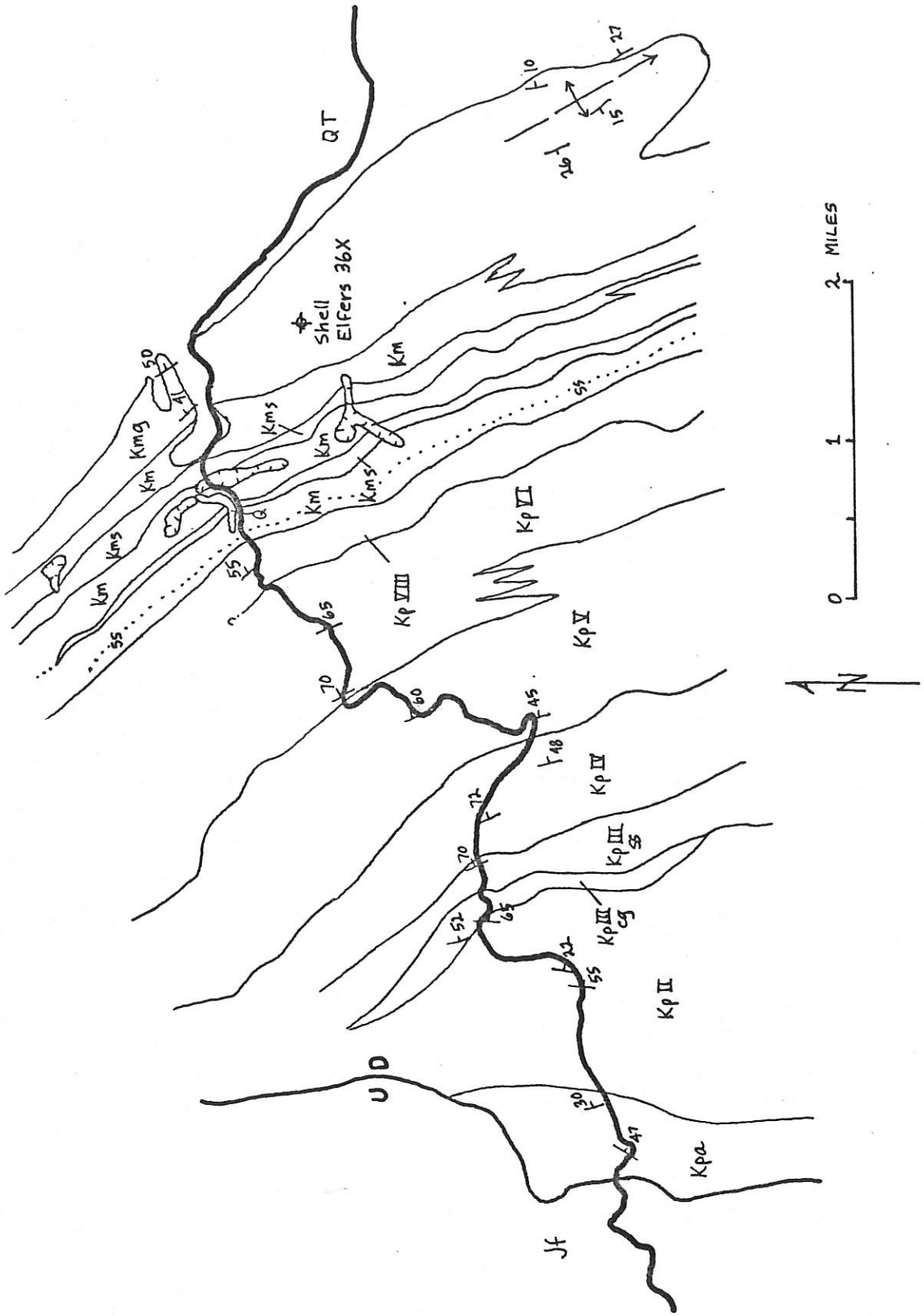


SKETCH MAP - DEL PUERTO CREEK CRETACEOUS SECTION, by CHARLES C. BISHOP

From SPECIAL REPORT 104, California Division of Mines and Geology, 1970
Plate 1

| COMPARATIVE NOMENCLATURE CHART — OLDER UNITS ← → YOUNGER UNITS | | | | | | | AUTHORITIES |
|---|---|---|---|---|---|---|---|
| KNOXVILLE? FORMATION[4] | | | | | | | |
| ADOBE FLAT SHALE MEMBER | PANOCHE FORMATION | | | MORENO FORMATION | | | MADDOCK (1964) (MT. BOARDMAN QUADRANGLE) |
| PACHECO GROUP | LOWER ASUNCION GROUP | | | UPPER ASUNCION GROUP | | | F.M. ANDERSON (1958) (EASTERN DIABLO RANGE) |
| | PANOCHE FORMATION | | | MORENO FORMATION | | | |
| | | | | MUSTANG | QUINTO | GARZAS (VOLTA)[3] | |
| HORSETOWN FORMATION[2] | PANOCHE FORMATION | | | MORENO GRANDE FORMATION | | | HUEY (1948) (TESLA QUADRANGLE) |
| PACHECO GROUP | ASUNCION GROUP | | | | | | TALIAFERO (1943) (EASTERN DIABLO RANGE) |
| | PANOCHE FORMATION | | | MORENO SHALE | | GARZAS SANDSTONE | |
| CHICO SERIES | | | | | | | F.M. ANDERSON (1943) (EASTERN DIABLO RANGE) |
| PIONEER GROUP | PANOCHE GROUP | | | MORENO GROUP | | | |
| | | | | MORENO | QUINTO | GARZAS | |
| CHICO GROUP | | | | | | | TAFF (1935) (MT. DIABLO AREA) |
| CHICO FORMATION | PANOCHE FORMATION | | | MORENO FORMATION | | | |
| CHICO GROUP | | | | | | | ANDERSON AND PACK (1915) (WEST SIDE SAN JOAQUIN VALLEY) |
| | PANOCHE FORMATION | | | MORENO FORMATION | | U. SDST. MBR. | |
| | PANOCHE FORMATION | | | MORENO FORMATION | | GARZAS MEMBER | SUBDIVISIONS OF THE CRETACEOUS ALONG DEL PUERTO CREEK AS USED IN THIS REPORT. |
| ADOBE FLAT SHALE MEMBER | II | III | IV | V | VI | VII | |
| H & G-2 | G-1 ZONE | F-2 ZONE | | F-1 ZONE | E ZONE | D-2 ZONE | C AND/OR D-1 ZONE | GOUDKOFF[1] (1945) |
| ALBIAN-TURONIAN | CONIACIAN-SANTONIAN | CAMPANIAN | | | | | MAESTRICHTIAN | EUROPEAN STAGES |
| LOWER CRET. | UPPER CRETACEOUS | | | | | | | SERIES |

1. Goudkoff's zones are applied to the subdivisions of the Upper Cretaceous from evidence obtained from microfossil localities in this area of this investigation.

2. Huey (1948) referred the Lower Cretaceous, Albian Stage rocks in the Tesla quadrangle to the Horsetown Formation.

3. The "Volta Sand" of Bennison referred to by Anderson (1958) is probably not present in the Del Puerto Creek area.

4. Although Upper Jurassic "Knoxville" beds are probably present at several localities in the Eastern Diablo Range, they are probably absent in the area covered by this report.

Figure 2. Comparison of nomenclature. The chart compares the subdivisions of this report with the nomenclature used by previous workers for the Cretaceous rocks exposed along the west side of the northern San Joaquin Valley.

**Figure 15. Correlation of the Measured Section Along Del Puerto Creek With the Shell Oil Company Elfers 36X-28 Well. The correlation shows the relationship of the subsurface nomenclature to the surface exposures.**

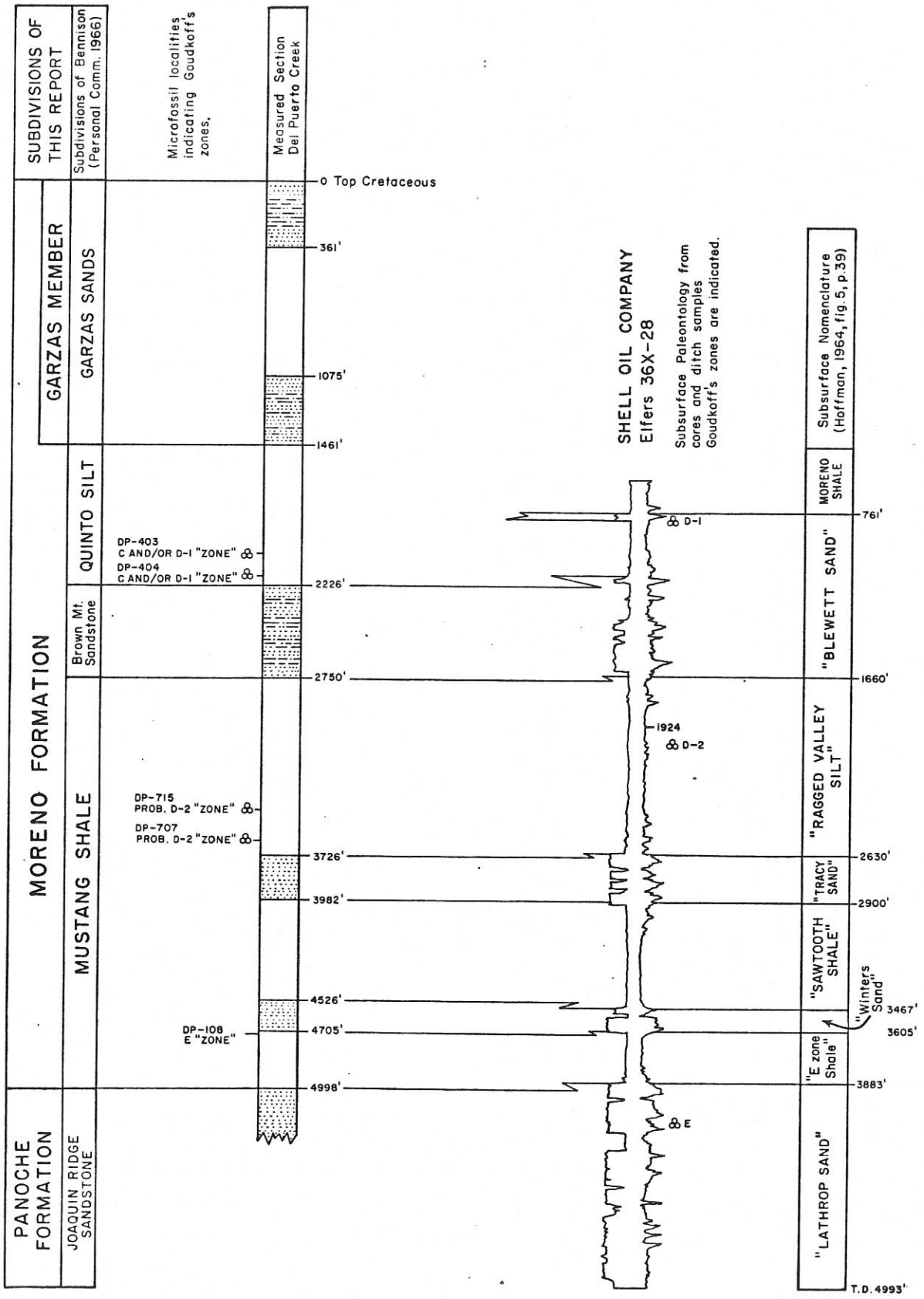

Table 1. Interpretation of typical elements of oceanic ophiolite sequences as displayed intact in overthrust oceanic slabs, as shreds in underthrust mélanges, and in varied disorder in suture zones formed by crustal collision. See text for discussion.

| Rock Types | Mode of Origin |
|---|---|
| B. CRUST ELEMENTS | |
| 7. Graywacke turbidites (not essential) | 7. Trench fills or subsea fans added just before subduction at convergent plate juncture. |
| 6. Chert and argillite (may be thin scum) | 6. Pelagic marine sediments added in transit from divergent to convergent plate juncture. |
| 5. Basaltic lavas and pillow lavas | 5. Sea-floor eruptions mainly where oceanic crust formed at midoceanic rise but partly younger seamounts. |
| 4. Dolerite screens and sills | 4. Feeders for rise eruptions where new lithosphere formed at divergent plate juncture. |
| 3. Varied gabbro bodies | 3. Supramantle magma chambers formed beneath midoceanic rise. |
| A. MANTLE ELEMENTS | |
| 2. Cumulus peridotite | 2. Remnants of magma chamber floors. |
| 1. Peridotite tectonite | 1. Refractory rind of residual outer mantle. |

Dickinson, 1971

# ON-LAND MESOZOIC OCEANIC CRUST IN CALIFORNIA COAST RANGES

By EDGAR H. BAILEY, M. C. BLAKE, JR.,
and DAVID L. JONES, Menlo Park, Calif.

*Abstract.*—The basal mudstones of the Upper Jurassic to Upper Cretaceous Great Valley sequence rest despositionally on a typical ophiolite ultramafic-mafic succession of igneous rocks. The ophiolite succession from top downward typically consists of chert; keratophyric to basaltic lavas; diabase, gabbro, or norite; and serpentinized peridotite, although not all parts are present everywhere. The volcanic rocks have an average thickness of 3,000 feet (900 m), and the serpentine may be as much as 5,000 feet (1,500 m) thick above a basal thrust fault. Comparison of occurrence, lithology, and thickness with the present in situ sea floor indicates that the ophiolite is the exposed Mesozoic oceanic crust on which sedimentary rocks of the Great Valley sequence were deposited. Coeval eugeosynclinal rocks of the Franciscan assemblage have been dragged below the rocks of the Great Valley sequence by sea-floor spreading. A great thrust fault, herein named the Coast Range thrust, separates the Franciscan and Great Valley sequence. Serpentine immeditaely above the thrust, previously thought to have been intruded into the fault zone, is the basal part of the Mesozoic oceanic crust lying beneath the Great Valley sedimentary rocks and thus was present before thrusting commenced.

The California Coast Ranges and adjacent Great Valley contain two coeval Upper Jurassic to Upper Cretaceous sequences, both possibly as much as 50,000 feet (15,000 meters) thick (see fig. 1). The western unit is the eugeosynclinal Franciscan assemblage of Bailey and others (1964), consisting of graywacke, shale, mafic volcanic rock, chert, limestone, and metamorphic rocks of zeolite and blueschist facies. The eastern unit is the Great Valley sequence, which consists predominantly of graywacke and shale with some conglomerate. This sequence was deposited in an area lying continentward from the site of accumulation of the eugeosynclinal Franciscan rocks, and it was referred to as miogeosynclinal by Bailey and others (1964) and as shelf and slope facies by Irwin (1964). Although its base is not exposed, the eugeosynclinal Franciscan assemblage has been regarded as having been deposited in a deep ocean environment on oceanic crust. In contrast, geologists have tended to regard the Great Valley sequence as having been deposited on continental crust because Cretaceous clastic strata of this sequence in the northern and eastern parts of the valley rest depositionally on the metamorphic and granitic rocks of the K[illegible]

## Mount Boardman

The ultramafic rocks of the Mount Boardman area (*5*, figs. 1 and 2) were described by Hawkes and others (1942), and a larger area was mapped in detail by Maddock (1964). Here beneath Jurassic shale of the Great Valley sequence is a typical ophiolite succession, but Maddock mapped major faults between some of the units. Beneath the Jurassic shale is his Lotta Creek Tuff Member, a unit 900 feet (275 m) thick consisting of mafic or keratophyric material with increasingly abundant siliceous shales or impure chert near the top. The tuff lies on a pile of keratophyre and quartz keratophyre flows 1,500 feet (450 m) thick with no sedimentary interbeds. Beneath the keratophyre, though everywhere mapped as separated by a fault, is hornblende gabbro cut by aplite, or perhaps trondjemite, dikes containing secondary prehnite. The gabbro in one area is in the center of a synclinal tabular mass of ultramafic rock, which we believe it overlies but which Maddock has separated by a fault. The sill-like ultramafic sheet is about 4,000 feet (1,200 m) thick and is largely serpentinized peridotite, although some dunite is present locally both near its base and top. The sheet is banded in places and contains segregations of chromite. It was mapped as intrusive into the Franciscan rocks by Maddock (1964), but its lower contact is shown as a fault by Hawkes and others (1942). We regard the surface below the serpentine as the major thrust fault that separates the Franciscan and Great Valley units.

U.S. GEOL. SURVEY PROF. PAPER 700–C, PAGES C70–C81

MT. BOARDMAN

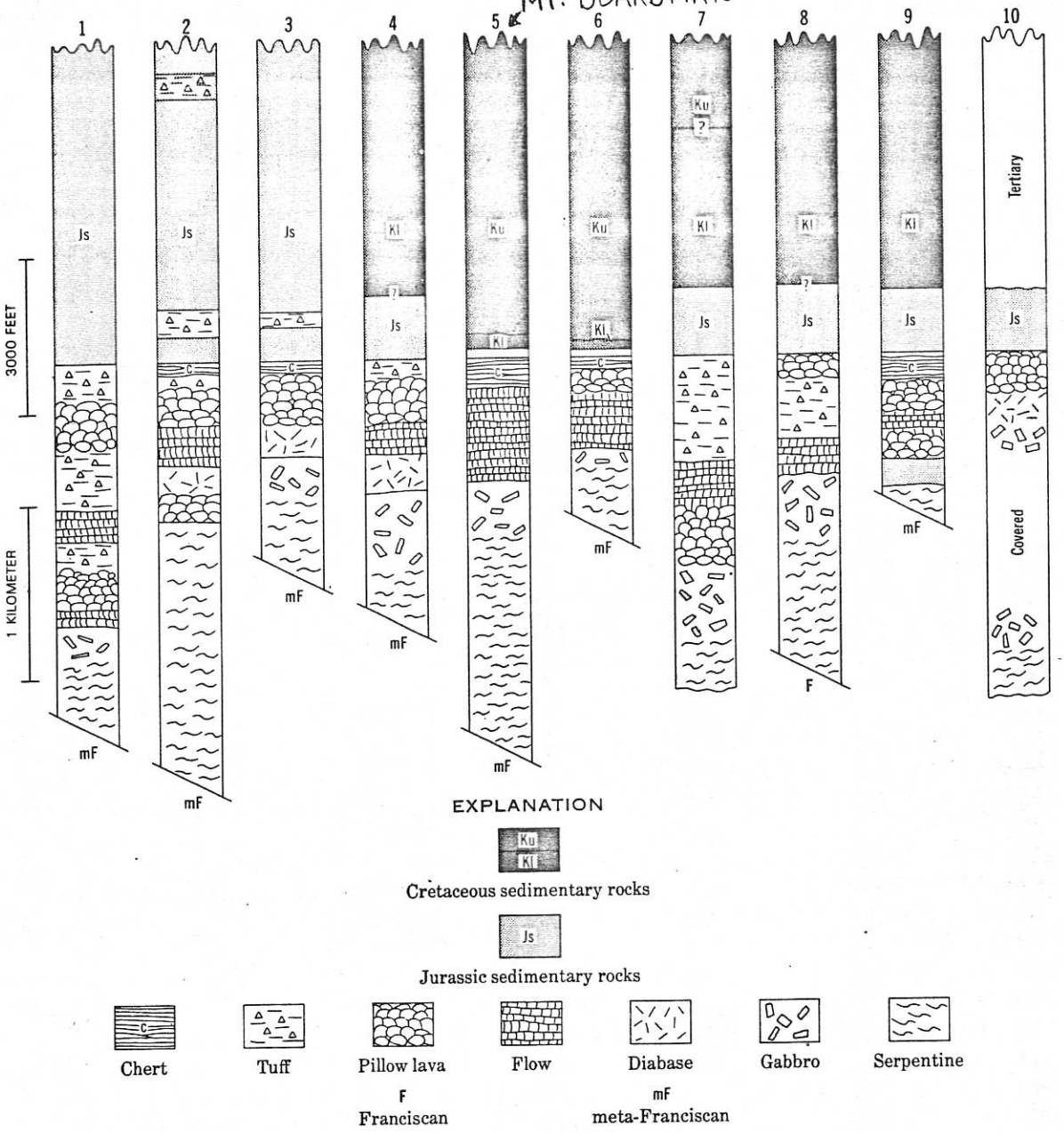


FIGURE 2.—Columnar sections showing details of the ophiolite succession at the numbered localities on figure 1

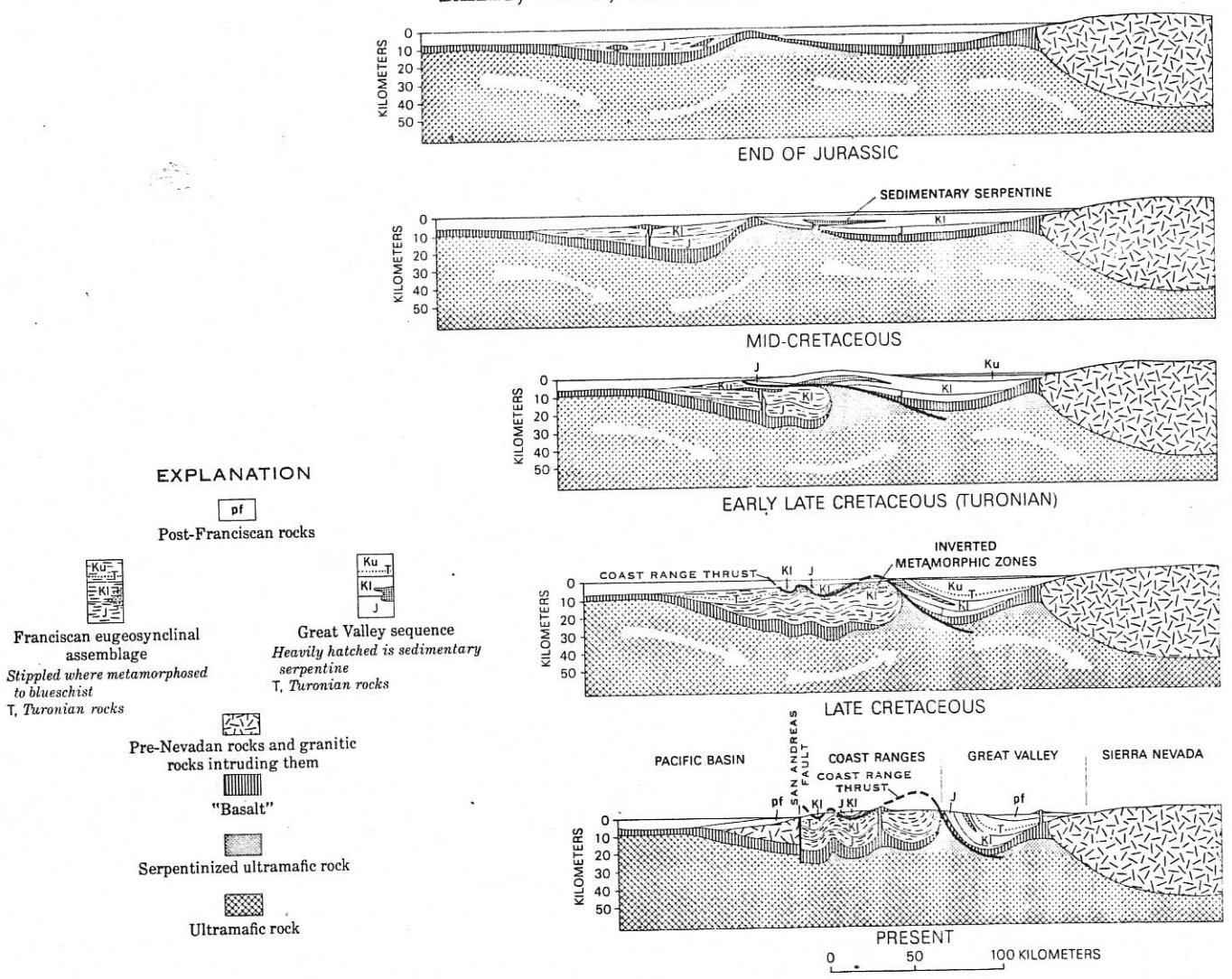


FIGURE 6.—Sequential sections through the Coast Ranges northeastward from a point on the coast 70 miles north of San Francisco. No attempt has been made to show the contemporaneous tectonism and intrusion in the Sierra Nevada block at right edge of sections or to show the complex structure within the Franciscan assemblage. Symbols: J, Jurassic; Kl, Lower Cretaceous; Ku, Upper Cretaceous.

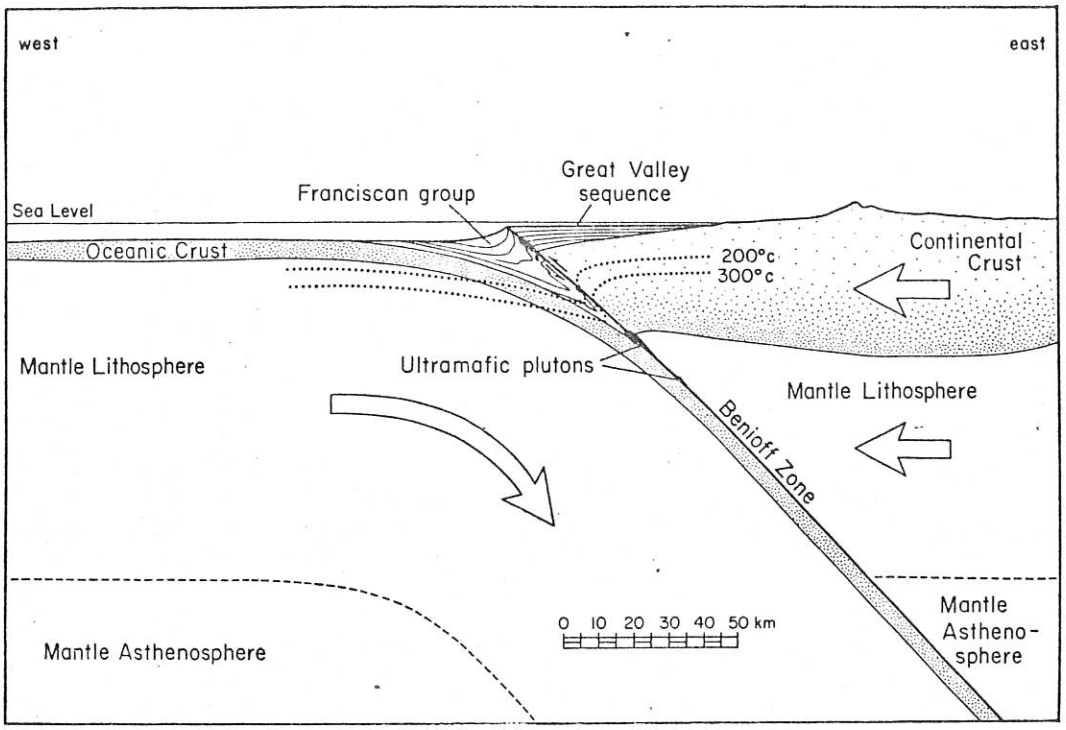


Fig. 3. Tectonic model involving deposition of the Franciscan mélange in a northwest-trending oceanic trench, and the Great Valley sequence principally on the adjacent continental slope and shelf. As illustrated, the Benioff zone in general marks the contact along which the continental lithospheric plate (continental crust plus mantle lithosphere) overrides the oceanic lithospheric plate (oceanic crust plus mantle lithosphere). Hydrated fragments of mantle material rise chiefly along this seismic shear zone, and are in part tectonically mixed into the trench mélange during deformation. No vertical exaggeration implied.

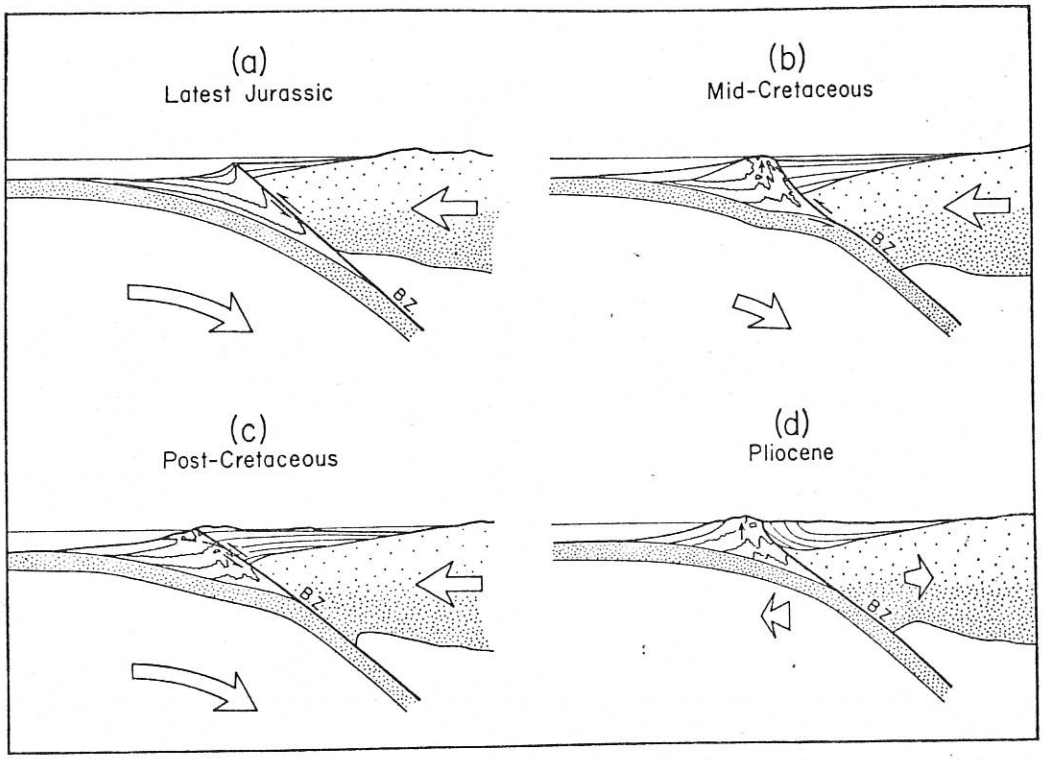


Fig. 4. Schematic models depicting stages of sea-floor spreading, and impingement of the continental lithosphere on the tectonically thickened and dragged down trench deposits (basically an elaboration on the central portion of Figure 3, same roughly east-west view). Arrow lengths indicate approximate relative convergence velocities; in (*d*), right-lateral movement is at a low angle to the plane of section; hence arrows are illustrated in perspective. Stages (*a*)–(*c*) are related to spreading presumably associated with nearby Late Mesozoic and Early Tertiary rises; in contrast, stage (*d*) depicts the modern movement picture involving the currently active East Pacific Rise. Geologic times indicated are only approximate. No vertical exaggeration implied.

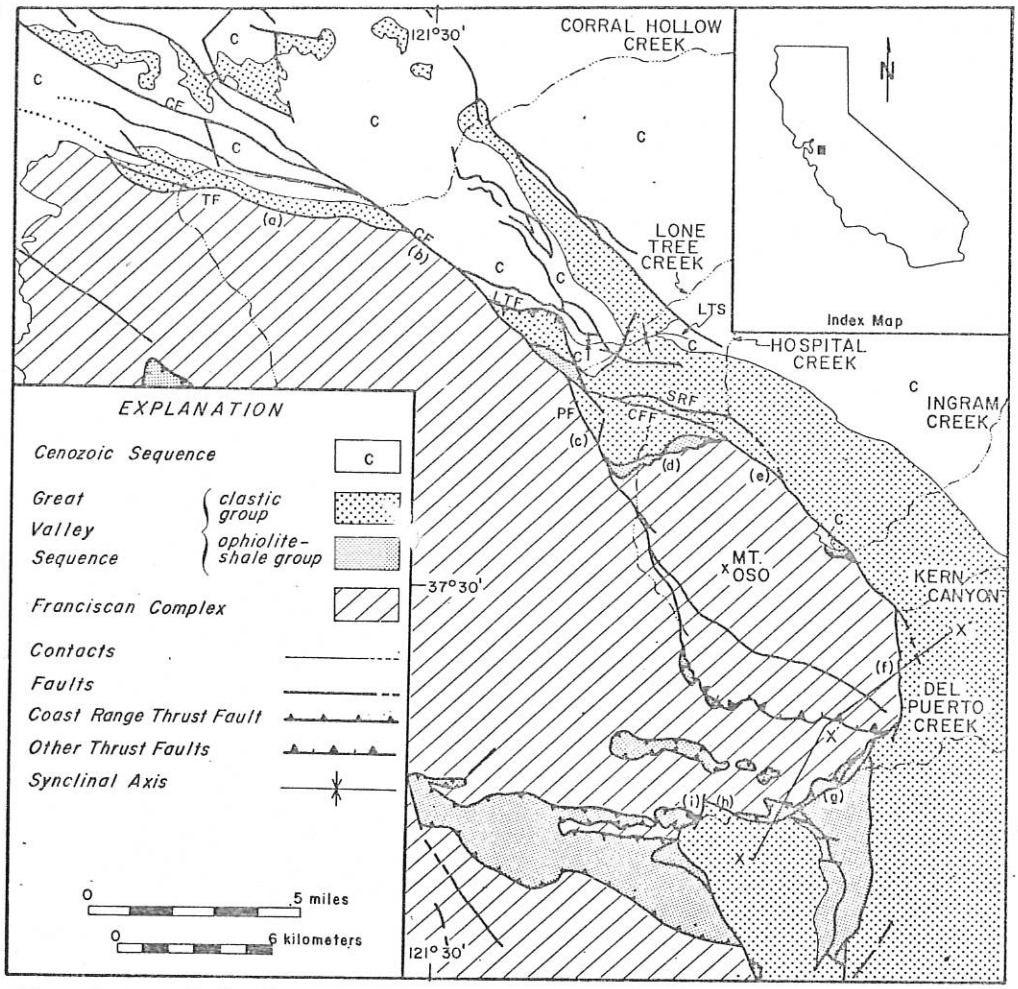


Figure 2. Generalized geologic map of the northeastern Diablo Range showing the general distribution of Franciscan, Great Valley sequence, and Cenozoic rocks. Lettered features include: TF, Tesla fault = (a); CF, Carnegie fault; LTF, Lone Tree fault, LTS, Lone Tree syncline; SRF, Seegers Ranch fault; CFF, Chicken Flat fault; PF, Pegleg fault; and (a) through (i), lettered segments of the Tesla-Ortigalita fault. Cross-section x-x'-x'' is shown in Figure 6. Southern part modified after Maddock, 1964.

thrust fault. Fault-affiliated deformation has deflected the axial trace of the Lone Tree syncline and has brought Cretaceous beds over overturned Cenozoic beds (Fig. 2). This deformation suggests contemporaneous right-lateral strike-slip movement of the Pegleg fault and thrusting on the Lone Tree fault. Because the Pegleg–Lone Tree fault cuts strata as young as late Miocene in age and truncates Great Valley sequence contacts at high angles, it is considered to be a Neogene fault that postdates the Coast Range thrust fault.

West of Hospital Creek (Fig. 2), the Pegleg fault truncates an older N. 70° E. trending fault segment designated (d). This fault dips from 42° to 70° northward. Great Valley sequence rocks in the hanging wall consist of the upper part of the ophiolite-shale group (Del Puerto and Lotta Creek Formations) and the overlying clastic group. Bedding is truncated at angles between 0° and 30°. The youngest beds cut by the fault belong to the middle Cretaceous Adobe Flat shale, only restricting the age of the fault to post-Turonian. The evidence therefore allows this fault to be considered a segment of the Coast Range thrust fault,

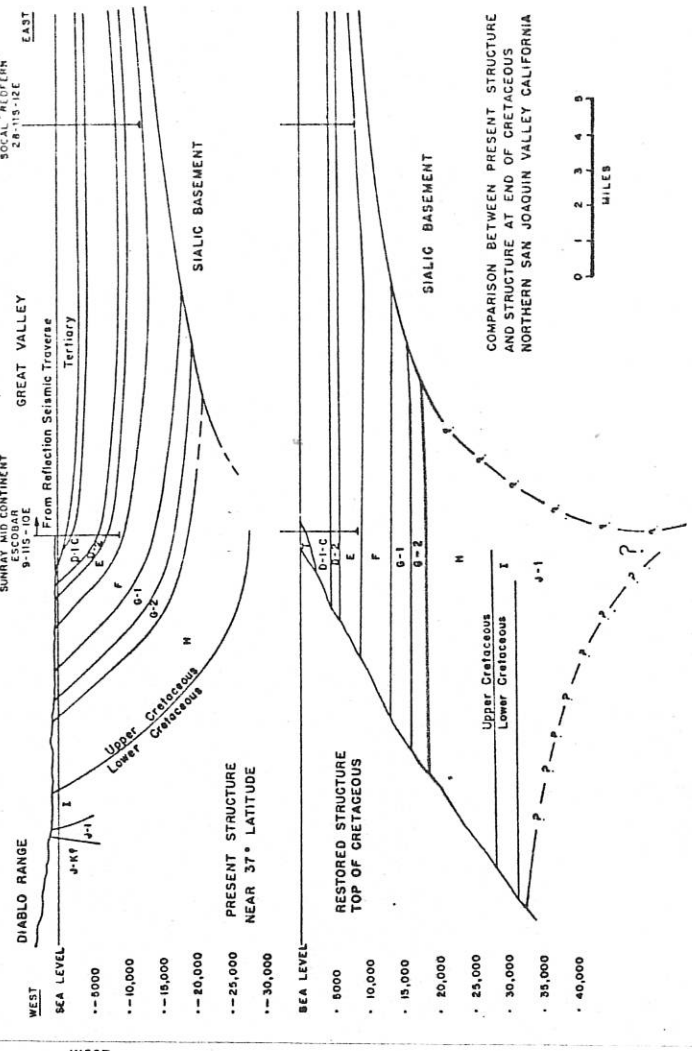


Figure 2. Upper: Cross section of boundary between the Coast Ranges and Great Valley at east side of Diablo Range. The Great Valley portion is the western end of a cross valley reflection seismic depth-section. Lower: Same cross section restored on top of Cretaceous, made horizontal. D-1C to J-1? are Cretaceous faunal zones.

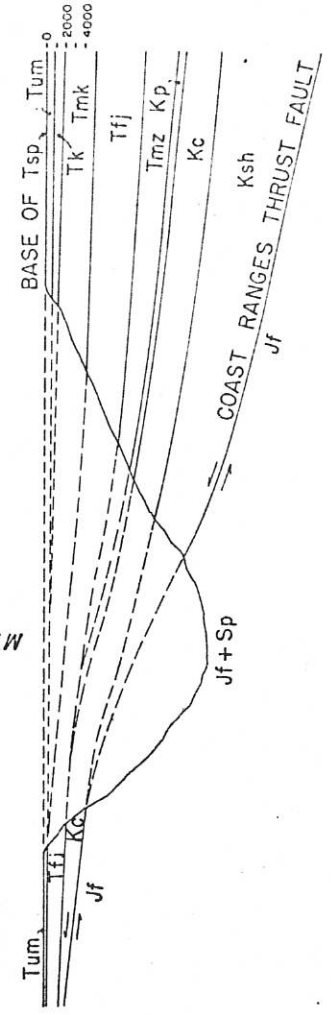


Figure 5. Restoration of cross section of Mt. Diablo anticline shown in Figure 4, by "unfolding" to make the base of the San Pablo Formation (T sp ) horizontal. The restoration shows evidence for the easterly (toward right-hand side) dip of the Coast Ranges thrust fault; for the mid-Eocene unconformity discussed in the text; and for a lower order of tectonism that continued in the Coast Ranges, after the Coast Ranges thrusting, and prior to the intense Plio-Pleistocene folding.

From W. F. Barbat (1971), GSA, v. 82, #6, pp. 1541-1562

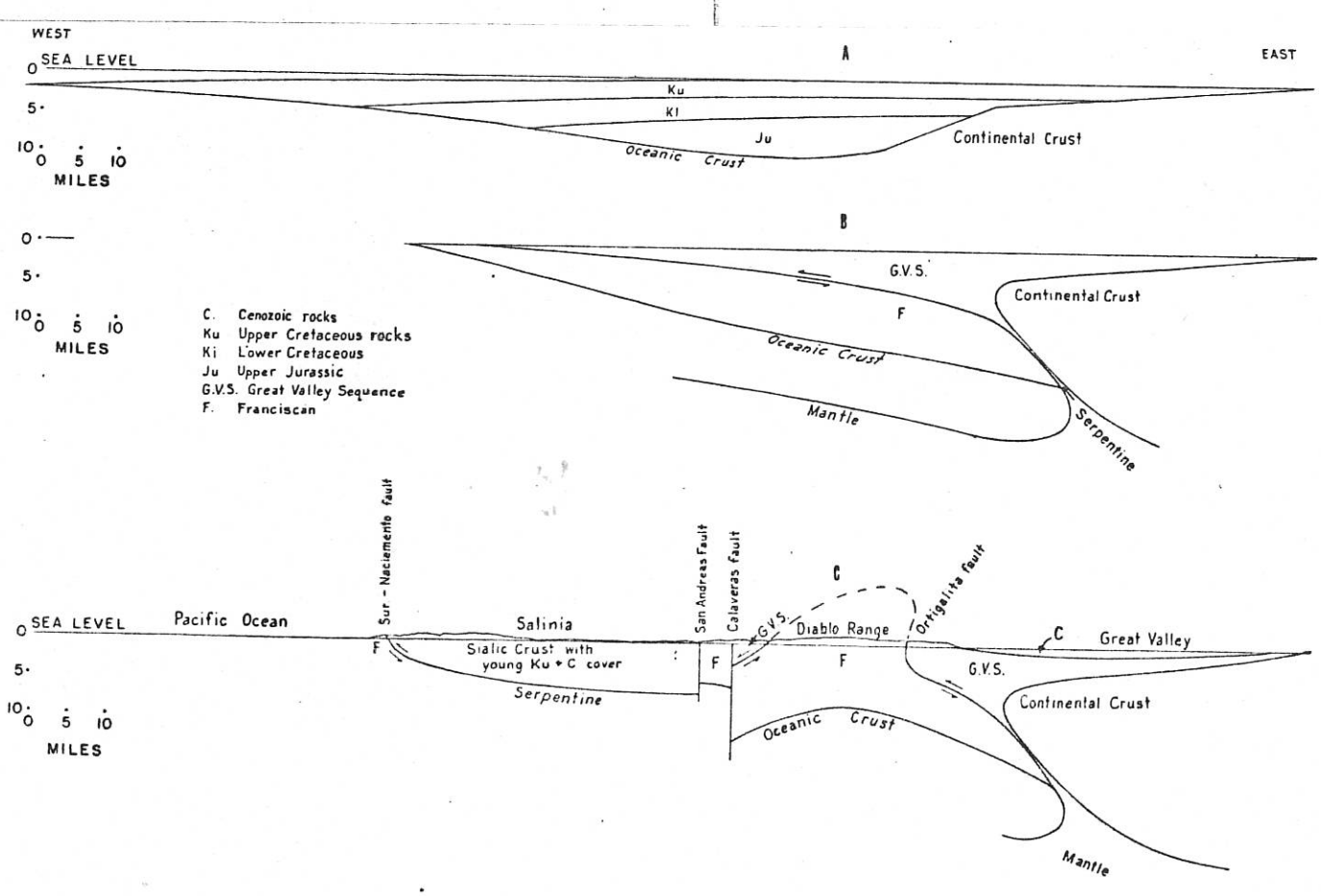


Figure 6. Model cross sections across the Coast Ranges. A. Prism of sedimentary rocks deposited from Late Jurassic to Late Cretaceous time across the boundary of oceanic and sialic crusts. B. The Coast Range orogeny showing a schematic representation of the Coast Ranges thrust. C. Post-Coast Ranges orogeny deformation, showing folding of the Coast Ranges thrust and right-lateral displacement on the San Andreas fault.

# DEL PUERTO CREEK

ontology

Section

Lithologic Description

en

0′

Unit designation
SAND, light gray, massive, friable to loose, medium to coarse grained, angular, silty to
up to 50% quartz, common dark rock grains, common biotite, common large scale cross b
occasional leaf impressions and pelecypods. Appears to be shallow or brackish water depos

361′

MORENO FORMATION
Garzas Sandstone Member
SANDSTONE, light to medium gray to locally dark gray, firm to friable on weathere
grained, in beds generally a foot to three feet thick, generally feldspathic with mino
metamorphic rock grains and rare red chert grains, common biotite locally altered to lim
clayey and locally calcareous, commonly very carbonaceous, grades upward into and is
SANDY SILTSTONE and SILTY SANDSTONE, medium gray to medium dark g
bedded to laminated with beds generally about three inches thick but occasional beds to
fine grained to locally fine to medium grained, scattered biotite, common carbonaceou
mentary structures such as load waves and pockets are common.

1,075′

SILTY CLAYSTONE, very poor outcropping, weathers to light to medium gray, comm
scattered finely divided biotite, possible forams.

1,461′

D-1 zone[9]

2,226′

SANDSTONE, light gray, in beds 10 to 15 feet thick, firm to friable, fine to medium
coarse grains, slump structures near base. Interbedded with:
SANDY CARBONACEOUS SILTSTONE, medium dark gray to brown, firm, in bed
feet thick, commonly clayey.

2,750′

bably D-2 zone

3,726′

3,982′

Unnamed Member
CLAYSTONE, medium chocolate brown, thinly bedded, firm, common carbonaceous m
staining on bedding planes, common lenses of gypsum, occasional forams.

4,526′

4,705′

4,998′

SANDSTONE: medium light dirty brownish gray on weathered surfaces, beds are genera
fine grained with occasional coarse grains, firm to friable, feldspathic, common medium
chert and quartzite, common coarse weathered biotite, silty, commonly calcareous, comm
few inches to several feet in diameter. Contains spherical bodies of shale a foot or two i
with SILTSTONE: medium brown weathering to light buff gray, in beds generally a
thickness but ranging to 25 or 30 feet, commonly fine grained sandy, locally grades to a si
brown with common gypsum and carbonaceous material, occasional cross laminations and
suggestive of a southeast to northwest current movement.

6,725′

CLAYSTONE, medium gray to chocolate brown, thinly bedded, commonly silty, comm
naceous material, scattered fish remains, locally common forams. And:
SANDSTONE, light gray to buff, thickly bedded to massive, firm to somewhat friable,
feldspathic, scattered biotite, common dark rock grains, principally quartzite, silty, local
calcareous and ferruginous concretions from a few inches to eight feet in diameter.

PANOCHE FORMATION
Unit VII
SANDSTONE, light gray weathering to buff, in beds from a few inches to three or fou
to friable, fine grained, feldspathic, common dark rock grains, principally gray and green c
common biotite and carbonaceous material, somewhat silty but appears to have fair to go
ability. Containing common laminae and thin interbeds of dark gray to black carbonace
ferruginous and calcareous concretions from a few inches to several feet in diameter, gene
elongated along the bedding planes. The lower half of the unit contains occasional interbe
feet in thickness of claystone, medium gray to brown, thinly bedded, firm, commonly silty
material, occasional *Inoceramus* fragments, common biotite, scattered forams. There is a
east alignment of sedimentary structures and cross laminations and erosional features i
from the northwest. Graded bedding can be seen on very close examination.

10,725′

Unit VI
SANDSTONE, light gray, in beds generally between two and 10 feet thick, firm to friab
sub-angular to sub-rounded, commonly poorly sorted, feldspathic, common biotite, occ
grains, rare carbonaceous material, somewhat silty. Common calcareous concretions that are
above, ranging from a few inches to a foot or so in diameter. Occasional laminae and thin in
of an inch to a foot or two in thickness of carbonaceous siltstone. Beds are graded upwar
complete.
The lower four hundred feet of the unit contains interbeds, a few feet in thickness, of clay
commonly fine grained sandy and silty, with common carbonaceous material.

# CHEMISTRY OF PRIMARY MINERALS AND ROCKS FROM THE RED MOUNTAIN–DEL PUERTO ULTRAMAFIC MASS, CALIFORNIA

By G. R. HIMMELBERG and R. G. COLEMAN, Menlo Park, Calif.

*Abstract.*—Rocks from the Red Mountain–Del Puerto ultramafic mass consist mainly of partly serpentinized harzburgite, dunite, and clinopyroxenite. Electron-microprobe and wet chemical analyses show that the compositional ranges of the primary silicate minerals from these rocks are small but can be related to sympathetic variations in bulk rock composition. Olivine from dunite and harzburgite is chemically homogeneous and ranges in composition from $Fo_{84.3}$ to $Fo_{90.9}$, whereas olivine from clinopyroxenite has a composition of $Fo_{75.5}$. Orthopyroxene ranges from $En_{90.0}$ to $En_{90.8}$ and has a small but significant range in $Al_2O_3$ content. Accessory chromian spinel shows a relatively large range in chemical composition, particularly in the Cr/Al ratio. Comparison of rock and primary mineral composition indicates that serpentinization occurred with minimal changes in rock chemistry, thereby requiring an appreciable volume increase of the serpentinized parts of the rocks.

The Red Mountain–Del Puerto ultramafic mass is on the eastern flank of the northwest-trending Diablo Range of northern California, where it occupies the axial part of the east-west trending Red Mountain syncline (fig. 1). According to Maddock (1964), the ultramafic mass is roughly tabular and has been folded after emplacement. Its contact against the surrounding Franciscan Formation of Jurassic and Cretaceous age is everywhere faulted or sheared, and its eastern part has been truncated by the Tesla-Ortigalita reverse fault, which separates the Franciscan Formation on the west from the Great Valley sedimentary sequence on the east. The Franciscan sedimentary and volcanic rocks are incipiently metamorphosed locally with the development of jadeite, lawsonite, and glaucophane (Maddock, 1964; Soliman, 1965). Glaucophane schists and related blueschist facies metamorphic rocks occur as small isolated tectonic blocks on the Franciscan erosional surface. Emplacement of the ultramafic mass and blueschist facies metamorphism may have been contemporaneous, but there is no direct evidence to substantiate contemporaneity. For a more extensive discussion of the regional and local geologic setting of the Red Mountain–Del Puerto ultramafic mass, the reader is referred to the studies of Hawkes, Wells, and Wheeler (1942), Bodenlos (1950), Maddock (1964), Soliman (1965), and Rogers (1965).

In contrast to most ultramafic masses of the Coast Ranges, which typically consist of highly sheared and completely serpentinized rocks, the Red Mountain–Del Puerto, Burro Mountain, and Cazadero ultramafic masses contain extensive areas of unserpentinized or only partly serpentinized primary rocks (Bailey and others, 1964). The purpose of this paper is to (1) establish the chemical, mineralogical, and petrological relationships between the ultramafic rocks of the Red Mountain–Del Puerto mass, and (2) evaluate the subsequent serpentinization in light of these relationships.

## PETROGRAPHY AND STRUCTURAL RELATIONSHIPS OF THE ULTRAMAFIC MASS

The Red Mountain–Del Puerto ultramafic mass consists primarily of harzburgite and dunite that are partly to completely serpentinized. Pyroxenite, gabbro, and wehrlite are present as minor bodies or dikes within the dunite and harzburgite. At the contact with the country rock, the ultramafic is generally sheared serpentinite containing coherent blocks of massive serpentinite that increase in size and number inward from the contact. The contact between the ultramafic rocks and the Franciscan rocks as shown in figure 1 should not be interpreted as an igneous contact. The sheared and serpentinized margin of the ultramafic body and the lack of a metamorphic aureole indicate that the Red Mountain–Del Puerto mass was tectonically emplaced as a cold, solid intrusion.

Zones of sheared and brecciated serpentinite also occur away from the contact areas and commonly contain magnesite or other carbonate minerals (hydromagnesite, aragonite, dolomite, and calcite; Ivan Barnes, oral commun., 1967). The magnesite in some occurrences has been mined, and a detailed discussion of these deposits is given by Bodenlos (1950).



U.S. GEOL. SURVEY PROF. PAPER 600-C, PAGES C18–C26

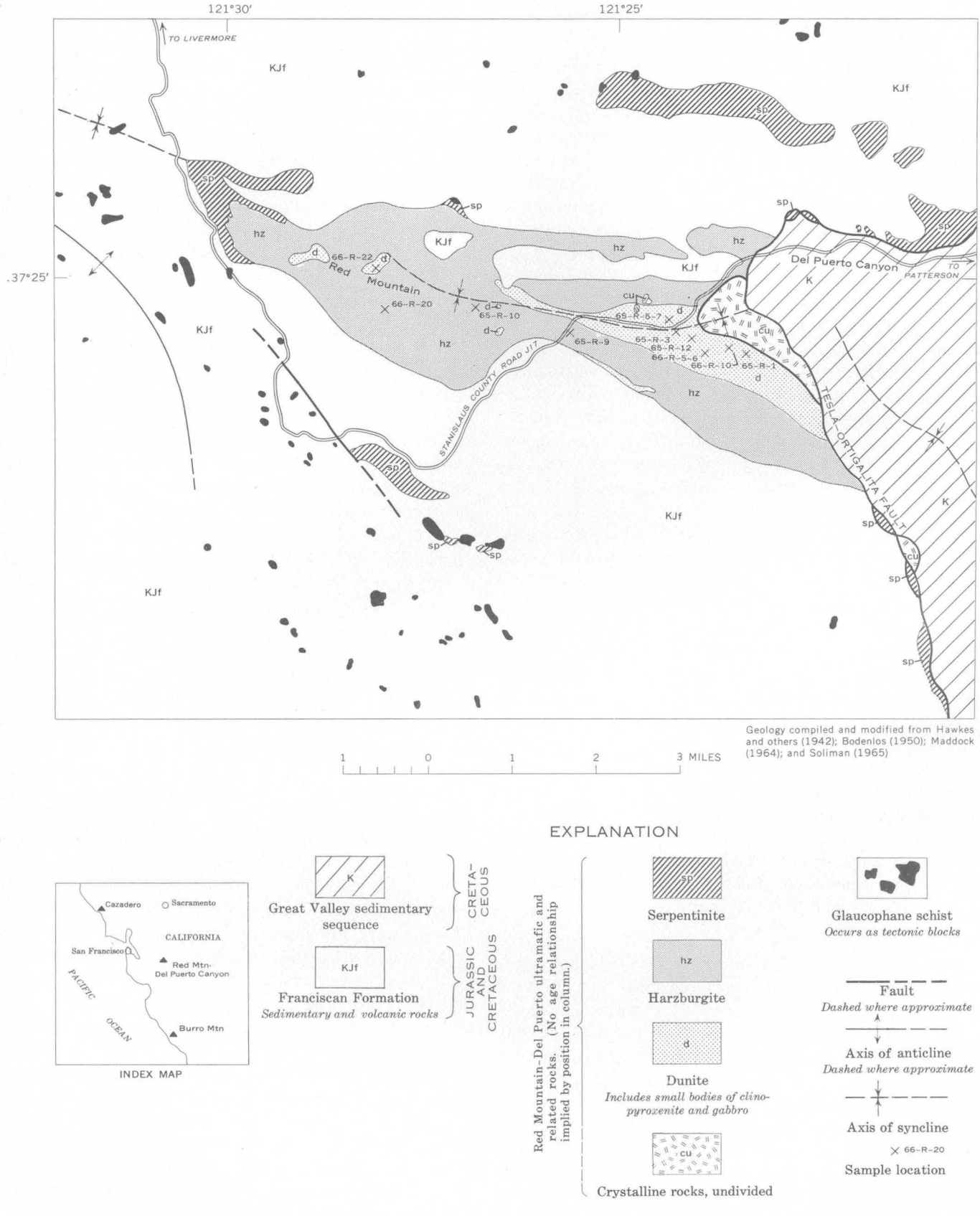


FIGURE 1.—Generalized geologic map of the Red Mountain–Del Puerto ultramafic mass and surrounding area.

### Harzburgite

The harzburgite is generally massive, except for local development of a crude foliation defined by alined pyroxene grains. The primary minerals in the harzburgite are olivine, orthopyroxene, and clinopyroxene, all of which occur as coarse, anhedral grains producing a granular interlocking fabric. Olivine, which generally has kink bands, and pyroxene are generally approximately equant; however, some of the smaller pyroxene grains appear to fill interstices. Orthopyroxene may exhibit undulatory extinction and bent cleavage traces and has fine lamellae, assumed to be exsolved diopside, parallel to (100). Accessory chromian spinel is subhedral to euhedral in some samples and anhedral in others. A modal analysis of one harzburgite sample (specimen 66–R–20) yielded the following mineral constituents (volume percent): olivine, 61.4; orthopyroxene, 27.2; clinopyroxene, 4.5; chromian spinel, 1.5; and serpentine, 5.4. Other harzburgite samples studied are more serpentinized, but their primary mineral content prior to serpentinization was probably similar to that of specimen 66–R–20.

Secondary minerals are abundant in the harzburgite, and were identified by optical, X-ray diffraction, and electron-microprobe techniques. Mesh-textured and bastite serpentine minerals (lizardite and minor chrysotile) coexisting with magnetite are ubiquitous. Brucite is a serpentinization product in some harzburgite samples. Replacement of pyroxene by tremolite is common, and textural evidence indicates that this process preceded serpentinization. A secondary mineral assemblage of talc, chlorite, and iron-rich serpentine (approximately 16 percent total iron as FeO) after orthopyroxene was observed in one sample. Antigorite is present locally in a zone at the top of Red Mountain; specimens containing antigorite also contain large, irregular magnetite grains and fibrous amphibole as narrow rims around pyroxene. Some specimens have chrysotile veins that cut the antigorite.

### Dunite

Contacts between the dunite and harzburgite are commonly sheared and appear to be steep. The dunite is massive, and the only megascopic structures associated with it result from disseminated chromite deposits that have narrow bands and lenses of chromitite alternating with dunite.

The dunite consists of coarse anhedral olivine producing a granular interlocking fabric, accessory euhedral to subhedral chromian spinel, and trace amounts of orthopyroxene and clinopyroxene. Kink bands of varied width are common in the olivine. Secondary minerals consist of mesh-textured serpentine (lizardite and minor chrysotile), brucite, and magnetite.

### Other rocks

Most pyroxenites in the ultramafic mass are clinopyroxenites that occur as veins and irregular "layers" and masses within other ultramafic rocks. At one locality clinopyroxenite is interlayered with harzburgite, and the interlayered pyroxenite-harzburgite is in turn enclosed in dunite. The clinopyroxenite layers range in thickness from several inches to 30 feet, and the trend of the layering is subparallel to the crude foliation in the harzburgite. Some small pyroxenite layers consist of alternating bands of orthopyroxene and clinopyroxene; one such layer, which has been folded, exhibits a well-developed foliation parallel to the axial plane of the fold.

Minerals of the clinopyroxenite are clinopyroxene and minor amounts of olivine, orthopyroxene, amphibole, and an opaque mineral. The rock has a medium to coarse granular texture. Orthopyroxene has fine lamellae of exsolved diopside parallel to (100). Clinopyroxene contains orthopyroxene lamellae and commonly exhibits bent cleavage traces. The only secondary mineral present is serpentine that rims olivine.

Orthopyroxenite veins and subparallel layers or dikes (generally less than 1 foot thick) of wehrlite in dunite are locally present but not common.

Two types of gabbro are present within the ultramafic body; olivine gabbro and a clinopyroxene-plagioclase gabbro. The olivine gabbro occurs near the eastern margin of the ultramafic mass as subparallel dikes as much as 3 feet thick cutting the dunite. The gabbro dikes are younger than clinopyroxenite veins in the dunite. Principal minerals are plagioclase ($An_{91}$), augite, olivine, and brown hornblende that replaces augite. The dike rocks have a crude banding, nematoblastic texture, and zones of cataclasis subparallel to the margins. The olivine is partly serpentinized. Foliated and lineated clinopyroxene-plagioclase gabbro occurs as a lenticular mass (75 to 100 feet thick) in sheared serpentinite near the eastern border of the ultramafic body. The primary minerals are clinopyroxene and plagioclase, and the texture of the rock is medium grained granular. Green hornblende partly replaces pyroxene, and the plagioclase is altered to hydrogrossular. Secondary prehnite, calcite, and chlorite are present in minor amounts.

The areas shown as "crystalline rocks undivided" on figure 1 were previously mapped as gabbro by Hawkes and others (1942) and by Maddock (1964), whereas these areas in fact contain poorly exposed amphibolite, volcanic rocks, porphyritic diorites, norite, aplite dikes, numerous quartz veins, and feldspathic peridotite. The contact between the ultramafic rocks and the "crystalline rocks undivided" is a fault contact (Hawkes and

others, 1942; Maddock, 1964), well delineated by sheared serpentinite.

In the explanation of figure 1, no age relationships are implied for the various ultramafic rocks and the crystalline rocks undivided. The gabbro dikes and at least some pyroxenites are later than the dunite, but no age relationships were established between the dunite and harzburgite. The crystalline rocks undivided may be genetically related to the Red Mountain–Del Puerto ultramafic rocks; however, poor exposures and tectonic juxtaposition preclude any definite determination. The serpentine is a result of alteration of dunite and harzburgite, a process that is probably still occurring (Barnes and others, 1967).

The nature of the primary crystallization of the Red Mountain–Del Puerto ultramafic rocks was not determined. The coarse-grained, interlocking fabric of the ultramafic rocks has none of the crystal settling textural characteristics described by Jackson (1961) for the Stillwater Complex, Montana. Moreover, the fabric, the presence of deformed olivine and pyroxene grains, and the small folds are more characteristic of metamorphic rocks than of igneous rocks, and it is possible that the existing fabric is a result of metamorphic recrystallization.

### Chemical composition of the ultramafic rocks

Rapid rock chemical analyses of dunite, harzburgite, clinopyroxenite, and gabbro are presented in table 1, spectrographic analyses of minor elements in table 2. The varied degree of serpentinization of the ultramafic rocks results in varied $H_2O$ content and introduces some difficulty in comparison of the analyses. The $Fe_2O_3$ content of the ultramafic rocks largely reflects the amount of magnetite, a byproduct of serpentinization. For calculation of the $\frac{Mg}{Mg+Fe+Mn}$ ratios in table 1, $Fe_2O_3$ was recalculated to FeO.

TABLE 1.—*Chemical analyses of ultramafic rocks and gabbro*

[Sample locations on figure 1. Chemical analyses after methods described by Shapiro and Brannock (1962), supplemented by atomic absorption analyses. Analysts: P. L. D. Elmore, Lowell Artis, G. W. Chloe, J. L. Glenn, S. C. Botts, H. Smith, Dennis Taylor, and S. M. Berthold]

| Constituent oxide | Dunite | | | | | Harzburgite | | | Clinopyroxenite [1] | Gabbro [2] | |
|---|---|---|---|---|---|---|---|---|---|---|---|
| | 65-R-1 | 65-R-3 | 65-R-12 | 66-R-6 | 66-R-22 | 65-R-9 | 65-R-10 | 66-R-20 | 65-R-7 | 66-R-5 | 66-R-10 |
| $SiO_2$ | 35.9 | 35.7 | 35.7 | 36.1 | 39.0 | 43.2 | 40.0 | 44.9 | 52.5 | 42.0 | 48.7 |
| $Al_2O_3$ | .43 | .19 | .28 | .76 | .04 | .58 | .58 | .91 | 1.2 | 11.0 | 15.0 |
| $Fe_2O_3$ | 4.5 | 5.3 | 3.8 | 3.7 | 2.8 | 1.7 | 3.2 | .80 | .70 | 2.1 | 1.0 |
| FeO | 3.7 | 4.9 | 3.2 | 4.5 | 5.0 | 5.6 | 4.0 | 7.0 | 5.0 | 7.6 | 3.8 |
| MgO | 42.2 | 41.3 | 42.6 | 41.7 | 46.1 | 41.5 | 41.8 | 43.0 | 20.6 | 19.3 | 10.8 |
| CaO | .30 | .22 | .30 | .85 | .00 | .73 | .30 | 1.5 | 18.8 | 12.0 | 15.7 |
| $Na_2O$ | .00 | .00 | .00 | .08 | .00 | .00 | .00 | .02 | .00 | .71 | 1.7 |
| $K_2O$ | .05 | .04 | .00 | .63 | .23 | .12 | .04 | .08 | .24 | .07 | .12 |
| $H_2O-$ | .65 | .55 | .57 | .45 | .50 | .16 | .65 | .09 | .11 | .32 | .19 |
| $H_2O+$ | 11.7 | 11.3 | 12.6 | 10.3 | 5.6 | 5.9 | 9.0 | 1.0 | .47 | 3.3 | 2.5 |
| $TiO_2$ | .02 | .00 | .00 | .02 | .02 | .02 | .00 | .02 | .00 | .82 | .29 |
| $P_2O_5$ | .07 | .07 | .06 | .03 | .03 | .06 | .06 | .03 | .06 | .04 | .02 |
| MnO | .14 | .18 | .12 | .12 | .11 | .15 | .12 | .12 | .18 | .16 | .09 |
| $CO_2$ | .32 | .34 | .24 | .08 | .21 | <.05 | .25 | <.05 | .05 | .16 | <.05 |
| NiO | .24 | .15 | .24 | .22 | .35 | .28 | .32 | .32 | .02 | .11 | .02 |
| $Cr_2O_3$ | .67 | .16 | .94 | .93 | .44 | .58 | .60 | .47 | .17 | .25 | .24 |
| Total | 100.9 | 100.4 | 100.6 | 100.5 | 100.4 | 100.6 | 100.9 | 100.3 | 100.1 | 99.9 | 100.2 |
| $SiO_2 : MgO$ | .85 | .86 | .84 | .87 | .85 | 1.04 | .96 | 1.04 | | | |
| Mole ratio $\frac{Mg \times 100}{Mg+Fe+Mn}$ | 90.6 | 88.1 | 91.9 | 90.4 | 91.5 | 91.1 | 91.4 | 90.8 | 86.3 | 78.1 | 80.2 |
| Density | 2.71 | 2.72 | 2.67 | 2.72 | 2.83 | 3.14 | 2.80 | 3.22 | 3.25 | 3.00 | 3.04 |
| Degree of serpentinization [3] | 78.5 | 77.0 | 83.5 | 77.0 | 62.5 | 19.5 | 66.5 | 10.0 | | | |

[1] Clinopyroxenite interlayered with harzburgite; harzburgite-pyroxenite enclosed in dunite.
[2] Specimen 66-R-5 is from an olivine gabbro dike that intrudes dunite. Specimen 66-R-10 is from a clinopyroxene-plagioclase gabbro lens in dunite.
[3] Based on density of rock by using 3.30 g/cc as density of fresh dunite and harzburgite, and 2.50 g/cc as density of serpentine.

## CHEMICAL COMPOSITION OF THE PRIMARY MINERALS

Analyses of primary minerals from dunite, harzburgite, clinopyroxenite, and gabbro are given in tables 3 through 6. Most analyses were made with a Materials Analysis Co. model-400 electron-microprobe analyzer using a 20 kilovolt excitation potential and a 0.0500-microampere specimen current. Intensities of $K\alpha$ X-ray lines were integrated over 20 seconds using potassium acid phthalate (KAP), ammonium dihydrogen phosphate (ADP), and LiF crystals and flow-proportional counters.

Mineral standards were used for analysis of all elements except for the minor elements Ni, Ti, and Cr, for which pure-element standards were used. All intensities

TABLE 2.—*Spectrographic analyses, in weight percent, of ultramafic rocks and gabbro*

[Sample locations on figure 1. Analyst: R. E. Mays. Abbreviation: n.d., not determined]

| Element | Dunite | | | | | Harzburgite | | | Clinopyroxenite [1] | Gabbro [2] | |
|---|---|---|---|---|---|---|---|---|---|---|---|
| | 65-R-1 | 65-R-3 | 65-R-12 | 66-R-6 | 66-R-22 | 65-R-9 | 65-R-10 | 66-R-20 | 65-R-7 | 66-R-5 | 66-R-10 |
| Al | 0.24 | 0.070 | 0.18 | 0.34 | 0.080 | 0.46 | 0.30 | 0.70 | 0.90 | n.d. | n.d. |
| Ba | <.0002 | <.0002 | <.0002 | <.0002 | <.0002 | .0006 | .0010 | <.0002 | .0002 | 0.0006 | 0.0022 |
| Ca | .16 | .11 | .18 | .80 | .050 | .80 | .26 | 1.8 | n.d. | n.d. | n.d. |
| Co | .0095 | .0095 | .010 | .010 | .011 | .013 | .0095 | .0075 | .0055 | .0065 | .0040 |
| Cr | .40 | .11 | .46 | .50 | .26 | .28 | .28 | .20 | .15 | .11 | .12 |
| Cu | .0008 | .0006 | .0004 | .0024 | .0008 | .0005 | .0005 | .0022 | .0007 | .017 | .018 |
| Mn | .10 | .11 | .090 | .060 | .060 | .10 | .090 | .10 | .14 | .10 | .065 |
| Ni | .22 | .10 | .20 | .14 | .21 | .24 | .24 | .18 | .017 | .065 | .018 |
| Sc | <.0008 | <.0008 | <.0008 | <.0008 | <.0008 | .0013 | <.0008 | .0018 | .0080 | .0055 | .0060 |
| Sr | | | | | | | | | | .020 | .036 |
| Ti | .0080 | .0015 | .0026 | .012 | .0008 | .0046 | .0018 | .0032 | .060 | .50 | .16 |
| V | .0019 | <.001 | .0019 | .004 | <.001 | .0044 | .0030 | .005 | .016 | .029 | .014 |

[1] Clinopyroxenite interlayered with harzburgite; harzburgite-pyroxenite enclosed in dunite.
[2] Specimen 66-R-5 is from an olivine gabbro dike intrusive into dunite. Specimen 66-R-10 is from a clinopyroxene-plagioclase gabbro lens in dunite.

TABLE 3.—*Chemical composition and structural formula of olivine from dunite, harzburgite, pyroxenite, and gabbro*

[Sample locations on figure 1. Electron-microprobe analyses by G. R. Himmelberg, except where otherwise indicated. Abbreviation: n.d., not determined]

| Constituents | Dunite | | | | | Harzburgite | | | | | Clino-pyroxenite | Gabbro |
|---|---|---|---|---|---|---|---|---|---|---|---|---|
| | 65-R-1 | 65-R-1 [1] | 65-R-3 | 66-R-6 | 66-R-22 | 65-R-5 | 65-R-9 | 65-R-9 [1] | 65-R-10 | 66-R-20 | 65-R-7 | 66-R-5 |
| **Chemical composition, in percent** | | | | | | | | | | | | |
| $SiO_2$ | 39.8 | 40.1 | 38.7 | 40.9 | 41.1 | 39.5 | 40.7 | 40.4 | 40.4 | 40.5 | 38.4 | 40.2 |
| $Fe_2O_3$ | | .2 | | | | | | .9 | | | | |
| FeO [2] | 9.8 | 8.5 | 12.7 | 9.3 | 8.9 | 15.6 | 9.8 | 8.5 | 9.2 | 10.1 | 19.6 | 22.9 |
| MgO | 49.8 | 49.8 | 48.2 | 49.9 | 50.9 | 46.4 | 49.4 | 49.6 | 49.2 | 50.1 | 42.9 | 39.4 |
| MnO | .2 | .14 | n.d. | .1 | .1 | n.d. | .1 | .13 | .1 | .1 | n.d. | .4 |
| NiO | .3 | .18 | n.d. | .3 | .3 | n.d. | .3 | .22 | .3 | .3 | n.d. | .04 |
| $H_2O+$ | n.d. | .56 | n.d. | n.d. | n.d. | n.d. | n.d. | .41 | n.d. | n.d. | n.d. | n.d. |
| $H_2O-$ | n.d. | .03 | n.d. | n.d. | n.d. | n.d. | n.d. | .02 | n.d. | n.d. | n.d. | n.d. |
| Total | 99.9 | 99.5 | 99.6 | 100.5 | 101.6 | 101.5 | 100.3 | 100.2 | 100.0 | 101.1 | 100.9 | 103.0 |
| **Structural formula, as number of cations per 4 oxygens** | | | | | | | | | | | | |
| Si | 0.98 | 0.99 | 0.97 | 1.00 | 0.99 | 0.98 | 1.00 | 0.99 | 1.00 | 0.99 | 0.98 | 1.01 |
| $Fe^{+3}$ | | .004 | | | | | | .02 | | | | |
| Mg | 1.83 | 1.83 | 1.80 | 1.81 | 1.82 | 1.72 | 1.80 | 1.81 | 1.81 | 1.82 | 1.63 | 1.48 |
| $Fe^{+2}$ | .20 | .18 | .26 | .19 | .18 | .32 | .20 | .17 | .19 | .21 | .42 | .48 |
| Mn | .004 | .003 | | .002 | .002 | | .002 | .003 | .002 | .002 | | .008 |
| Ni | .006 | .004 | | .006 | .006 | | .006 | .004 | .006 | .006 | | .001 |
| Sum of two valent cations. | 2.04 | 2.02 | 2.06 | 2.01 | 2.01 | 2.04 | 2.01 | 1.99 | 2.01 | 2.03 | 2.05 | 1.97 |
| $\frac{Mg \times 100}{Mg+Fe+Mn}$ | 90.0 | 90.7 | 87.4 | 90.4 | 90.9 | 84.3 | 89.9 | 90.4 | 90.4 | 89.6 | 79.5 | 75.2 |

[1] Wet chemical analysis by Marcelyn Cremer.
[2] Total iron computed as FeO for electron-microprobe analyses

were corrected for background and instrument drift. Absorption corrections were made using Philibert's (1963) formula for $f(\chi)$ as modified by Duncumb and Shields (1966). Heinrich's (1966) mass absorption coefficients were used. The geometrical factor 1.6071 was used in the absorption correction for the expression $\text{cosec}\theta \sin\phi$, where $\theta$ refers to the X-ray takeoff angle and $\phi$ refers to the electron beam angle of incidence. Data corrected for absorption were refined to 0.1 weight percent of the elements.

The microprobe analyses given are averages of determinations on 5 to 10 points per grain, using 4 or 5 grains per sample. The precision of a single point determination (one standard deviation) is within 2 percent of the amount of the element present. The concentration of total iron was computed as FeO.

Pure mineral separates for standard chemical analyses were obtained from −200 to+325 mesh material by means of centrifuging in heavy liquids and by use of the Frantz isodynamic magnetic separator. Structural

TABLE 4.—*Spectrographic analyses, in weight percent, of olivine and pyroxene*

[Analyst: R. E. Mays. Abbreviation: n.d., not determined, major element]

| Element | Olivine (in dunite, 65-R-1) | Olivine (in harzburgite, 65-R-9) | Clinopyroxene (in clinopyroxenite, 65-R-7) |
|---|---|---|---|
| Al | 0.005 | 1.007 | 0.70 |
| Ca | .020 | .014 | n.d. |
| Co | 0.14 | .014 | .0030 |
| Cr | .0080 | .0085 | .10 |
| Cu | .0006 | .0030 | .0032 |
| Mn | .12 | .12 | .12 |
| Ni | .14 | .17 | .010 |
| Sc | <.0002 | <.0002 | .010 |
| Ti | .0008 | <.0004 | .055 |
| V | <.001 | <.001 | .020 |

TABLE 5.—*Chemical composition and structural formula of pyroxene from harzburgite and clinopyroxenite*

[Sample locations on figure 1. Electron-microprobe analyses by G. R. Himmelberg, except where otherwise indicated. Abbreviation: n.d., not determined]

| Constituent oxides and elements | Orthopyroxene | | | Clinopyroxene | |
|---|---|---|---|---|---|
| | 65-R-9 [1] | 65-R-10 [1] | 66-R-20 [1] | 66-R-20 [1] | 65-R-7 [2,3] |
| **Chemical composition, in percent** | | | | | |
| $SiO_2$ | 56.7 | 57.5 | 55.2 | 52.5 | 53.4 |
| $Al_2O_3$ | 1.0 | .7 | 2.8 | 2.0 | 1.1 |
| $Fe_2O_3$ | | | | | .5 |
| FeO [4] | 5.8 | 5.9 | 6.2 | 2.0 | 3.2 |
| MgO | 35.0 | 36.2 | 35.2 | 17.9 | 17.5 |
| CaO | .7 | .5 | .6 | 24.8 | 23.6 |
| MnO | .1 | .1 | .2 | | .13 |
| $Cr_2O_3$ | .3 | n.d. | .5 | .6 | .15 |
| $TiO_2$ | | | | .02 | |
| $H_2O+$ | n.d. | n.d. | n.d. | n.d. | .22 |
| $H_2O-$ | n.d. | n.d. | n.d. | n.d. | .04 |
| Total | 99.6 | 100.9 | 100.7 | 99.8 | 99.6 |
| **Structural formula, as number of cations per 6 oxygens** | | | | | |
| Z Si | 1.96 | 1.96 | 1.90 | 1.92 | 1.96 |
| Z $Al^{IV}$ | .04 | .03 | .10 | .08 | .04 |
| X, Y $Al^{VI}$ | .003 | | .01 | .004 | .005 |
| X, Y Ti | | | | .001 | |
| X, Y Cr | .008 | | .014 | .02 | .004 |
| X, Y $Fe^{+3}$ | | | | | .01 |
| X, Y Mg | 1.80 | 1.84 | 1.80 | .97 | .96 |
| X, Y $Fe^{+2}$ | .17 | .17 | .18 | .06 | .10 |
| X, Y Mn | .003 | .003 | .006 | | .004 |
| X, Y Ca | .03 | .018 | .02 | .97 | .93 |
| Sum X, Y group | 2.01 | 2.03 | 2.03 | 2.02 | 2.01 |
| Atomic ratios | | | | | |
| Mg | 90.3 | 90.8 | 90.0 | 48.6 | 48.3 |
| Fe | 8.4 | 8.3 | 8.9 | 3.0 | 4.9 |
| Ca | 1.3 | .9 | 1.1 | 48.4 | 46.8 |
| $\frac{Mg \times 100}{Mg+Fe+Mn}$ | 91.20 | 91.4 | 90.6 | 94.1 | 90.2 |

[1] From harzburgite.
[2] From clinopyroxenite.
[3] Wet chemical analysis by Marcelyn Cremer.
[4] Total iron computed as FeO for probe analyses.

formulas were calculated by the hydrogen-equivalent method (Jackson and others, 1967).

## Olivine

Tables 3 and 4 give the chemical composition, mineral formula, and minor-element content of olivine from some rocks of the Red Mountain–Del Puerto mass. Most of the chemical compositions were determined by electron-microprobe techniques; however, olivine from two samples (65–R–1, 65–R–9) was also analyzed by standard wet chemical methods for comparison. Agreement between the two methods is within 1 percent of the amount present for MgO and $SiO_2$; but total iron shows a significant difference for olivine from sample 65–R–1. The analysis of olivine from sample 66–R–5 (table 1) contains a significant error that is probably a result of no correction for fluorescence, as there is a large compositional difference between the sample ($Fo_{75}$) and the standard ($Fo_{91}$).

The electron-microprobe analyses of olivine show them to be chemically homogeneous; there are no measurable compositional differences from grain to grain and no zoning within individual grains. In general, the standard deviation from the average composition is less than 2 percent of the amount present, which is within the analytical precision of the analyses. The maximum relative standard deviation was 3.5 percent for $SiO_2$ in one sample.

Analyzed olivine from dunite and harzburgite has a small range in composition, $Fo_{84.3}$ to $Fo_{90.9}$. The harzburgite with olivine of composition $Fo_{84.3}$ is interlayered with clinopyroxenite that has an olivine of $Fo_{79.5}$ composition. The most iron-rich olivine analyzed (approximately $Fo_{75}$) is from an olivine gabbro dike that intrudes dunite.

The range in composition of olivine ($Fo_{84.3}$ to $Fo_{90.9}$) from dunite and harzburgite from the Red Mountain–Del Puerto ultramafic mass is similar to the compositional range of olivine from other alpine-type peridotites, which, as compiled by Green (1964), is typically $Fo_{88}$ to $Fo_{93}$.

## Orthopyroxene

Table 5 shows that the three orthopyroxenes analyzed have a range in composition from $En_{90.0}$ to $En_{90.8}$, which is within the precision of the analytical method and is typical of the compositional range of orthopyroxene from other alpine-type peridotites (Ross and others, 1954; Green, 1964; Challis, 1965; Page, 1967). The distribution of the major elements Si, Mg, and Fe is chemically homogeneous within analytical precision.

The CaO content (less than 1 percent) of the orthopyroxene is lower than generally reported for orthopyroxenes from other alpine-type peridotites (Ross and others, 1954; Green, 1964; Challis, 1965). The presence of clinopyroxene exsolution lamellae, however, indicates that calcium was removed from the orthopyroxene structure during cooling, and the microprobe analyses do not fully account for these lamellae nor the original calcium content of the orthopyroxenes. Howie and Smith (1966, p. 454) have shown that, in general, microprobe analyses of orthopyroxene yield lower values for calcium than do wet chemical analyses. The calcium distribution in the orthopyroxene as determined with the electron microprobe is irregular and is probably a result of the clinopyroxene exsolution lamellae being partly included for some determination points.

Aluminum is irregularly distributed in a single orthopyroxene grain and shows a significant difference between orthopyroxene samples. The bulk composition control for the variation can be seen by comparing the $Al_2O_3$ content of the orthopyroxenes with the $Al_2O_3$ content of the whole rock. For example, the orthopyroxene with the highest $Al_2O_3$ content (sample 66–R–20, 2.8 percent $Al_2O_3$) is from the harzburgite with the highest $Al_2O_3$ content (0.91 percent $Al_2O_3$, table 1) and coexists with an aluminium-rich chromian spinel (36.2 percent $Al_2O_3$, table 6).

Nickel and titanium were looked for with the microprobe but were not detected.

### Clinopyroxene

Table 5 shows that clinopyroxene from the clinopyroxenite (sample 65–R–7) is significantly higher in iron content than the clinopyroxene from the harzburgite (sample 66–R–20); similarly, in the same specimens the olivine from the clinopyroxenite is higher in iron content than olivine from the harzburgite (see table 3). The other major differences are higher $Al_2O_3$ and $Cr_2O_3$ contents in the clinopyroxene from the harzburgite.

The clinopyroxene from the harzburgite has a higher $\frac{Mg}{Mg+Fe+Mn}$ ratio and a lower $Al_2O_3$ content compared with the coexisting orthopyroxene. The two coexisting pyroxenes, however, have similar $Cr_2O_3$ contents. Spectrographic analysis for clinopyroxene from the clinopyroxenite (sample 65–R–7) is given in table 4.

### Chromian spinel

In contrast to the primary silicate minerals, the chromian spinels show a considerable range in chemical composition (table 6), particularly in Cr/Cr+Al ratio (fig. 2). Irvine's (1967) compilation of chromian spinel compositions from other alpine-type peridotites shows similar variations. Also unlike the silicate minerals, individual spinel grains show significant chemical inhomogeneity for all elements analyzed (±5 to 10 percent of the average amount present).

TABLE 6.—*Chemical composition and structural formula of chromian spinel*

[Sample locations on figure 1. All analyses made with electron microprobe by G. R. Himmelberg]

| Constituent oxides and elements | Dunite | | | Harzburgite | |
|---|---|---|---|---|---|
| | 65–R–1 | 66–R–6 | 66R–22 | 65–R–9 | 66–R–20 |
| **Chemical composition, in percent** | | | | | |
| $Cr_2O_3$ | 41.5 | 42.0 | 56.3 | 50.7 | 27.9 |
| $Al_2O_3$ | 17.8 | 15.2 | 7.4 | 11.4 | 36.2 |
| $Fe_2O_3$[1] | 10.1 | 12.0 | 7.2 | 6.7 | 3.2 |
| FeO | 20.5 | 21.6 | 21.7 | 22.2 | 12.7 |
| MgO | 9.1 | 8.1 | 7.5 | 7.2 | 15.4 |
| Total | 99.0 | 98.9 | 100.1 | 98.2 | 95.4 |
| **Structural formula, as number of cations per 32 oxygens** | | | | | |
| Cr | 8.55 | 8.83 | 12.14 | 10.95 | 5.26 |
| Al | 5.47 | 4.76 | 2.38 | 3.67 | 10.17 |
| $Fe^{+3}$ | 1.98 | 2.40 | 1.48 | 1.38 | .57 |
| $Fe^{+2}$ | 4.47 | 4.80 | 4.95 | 5.07 | 2.53 |
| Mg | 3.53 | 3.21 | 3.05 | 2.93 | 5.47 |
| Sum $R^{+3}$ | 16.00 | 15.99 | 16.00 | 16.00 | 16.00 |
| Sum $R^{+2}$ | 8.00 | 8.01 | 8.00 | 8.00 | 8.00 |
| $\frac{Cr\times100}{Cr+Al}$ | 61.0 | 65.0 | 83.6 | 74.9 | 34.1 |
| $\frac{Fe^{+3}\times100}{Fe^{+3}+Cr+Al}$ | 12.4 | 15.0 | 9.2 | 8.6 | 3.6 |
| $\frac{Mg\times100}{Mg+Fe^{+2}}$ | 44.1 | 40.1 | 38.1 | 36.6 | 68.4 |

[1] Calculated from total iron by assuming $RO/R_2O_3$ ratio of 1/1, and the structural formula was calculated on this basis.

Although not compelling, the data suggest a possible correlation between texture and chemical composition. The most aluminum-rich spinel (36.2 percent $Al_2O_3$, sample 66–R–20) occurs in harzburgite as anhedral grains, some of which appear to be interstitial, whereas the other four analyzed chromian spinels contain less than 20 percent $Al_2O_3$ and occur as subhedral to euhedral grains. Moreover, the most aluminum-rich chromian spinel coexists with the most aluminum-rich orthopyroxene analyzed.

## SERPENTINIZATION

The effect of serpentinization on the chemical composition of the Red Mountain–Del Puerto ultramafic rocks can be partly evaluated by comparing the rock composition, mineral composition, and degree of serpentinization. The density of both olivine of composition $Fo_{90}$ and orthopyroxene of composition $En_{90}$ is approximately 3.30 g/cc, and the density of serpentine is about 2.50 g/cc; therefore, the density of dunite and

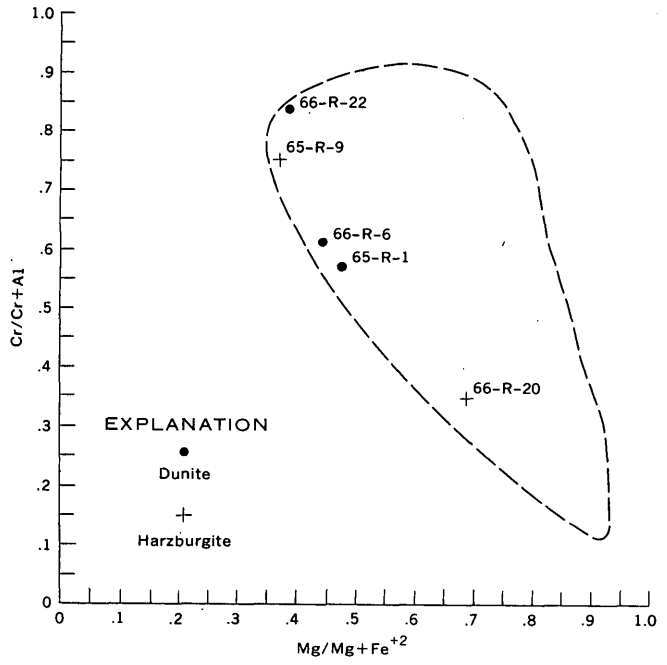


FIGURE 2.—Cr/Cr+Al and Mg/Mg+Fe$^{+2}$ ratios of accessory chromian spinels from rocks of the Red Mountain–Del Puerto ultramafic mass. Outlined area is approximate field of composition of chromian spinels from other alpine-type peridotites as shown by Irvine (1967). Sample localities shown on figure 1.

harzburgite composed mainly of olivine and orthopyroxene can be used as an approximate index of serpentinization (table 1).

In table 7, the molecular ratio $\frac{Mg\times100}{Mg+Fe+Mn}$ is compared for olivine, orthopyroxene, and whole rock. For calculation of the $\frac{Mg\times100}{Mg+Fe+Mn}$ ratio of whole rock, the Fe$^{+3}$ present was assumed to be largely from magnetite produced during serpentinization and was recalculated to Fe$^{+2}$. Within analytical error, the $\frac{Mg\times100}{Mg+Fe+Mn}$ ratio of the olivine is the same as for the orthopyroxene in the same rock. Because these two minerals composed nearly all of the original rock, their $\frac{Mg\times100}{Mg+Fe+Mn}$ ratio in effect determines the $\frac{Mg\times100}{Mg+Fe+Mn}$ ratio of the primary rock. In view of the fact that these rocks are largely serpentinized (except for harzburgite 66–R–20; see table 1), the close agreement between the $\frac{Mg\times100}{Mg+Fe+Mn}$ ratio of the whole rock and of the contained minerals indicates that serpentinization of these rocks proceeded under conditions that maintained a nearly constant $\frac{Mg\times100}{Mg+Fe+Mn}$ ratio.

TABLE 7.—*Comparison of mole ratio,* $\frac{Mg\times100}{Mg+Fe+Mn}$, *for whole rock and coexisting olivine and orthopyroxene*

| Sample | Whole rock [1] | Olivine | Orthopyroxene |
|---|---|---|---|
| 65–R–1 | 90.6 | 90.0 | ---------- |
| 65–R–3 | 88.1 | [2] 87.4 | ---------- |
| 66–R–6 | 90.4 | 90.4 | ---------- |
| 66–R–22 | 91.5 | 90.9 | ---------- |
| 65–R–9 | 91.1 | 90.4 | 91.2 |
| 65–R–10 | 91.4 | 90.4 | 91.4 |
| 66–R–20 | 90.8 | 89.6 | 90.6 |

[1] $Fe_2O_3$ converted to FeO.
[2] Mn not determined. Ratio is $\frac{Mg\times100}{Mg+Fe}$.

A dunite consisting mainly of olivine of composition $Fo_{90}$ should have an $SiO_2/MgO$ ratio of approximately 0.83, and if serpentinization proceeds under conditions of constant chemical composition, this ratio should not change appreciably. Table 1 shows that the $SiO_2/MgO$ ratios of the dunites are slightly larger than 0.83 and range from 0.84 to 0.87. The differences between the dunite and olivine $SiO_2/MgO$ ratios are small, and because there is no correlation with degree of serpentinization, it is possible that the differences are due to analytical errors.

If, however, the differences between dunite and olivine $SiO_2/MgO$ ratios are real, then the increased ratio of the dunites could be due to addition of silica or removal of magnesia during serpentinization. If it is assumed that there was no addition of silica, the $SiO_2/MgO$ ratios of the dunites require that approximately 1 to 5 mole percent of the original magnesia was removed from the dunites during serpentinization. Migration of this amount of magnesia is comparable to the findings of Hostetler, Coleman, Mumpton, and Evans (1966, p. 91) for other serpentinized dunites. An alternative explanation for the $SiO_2/MgO$ ratios of the dunites is that they originally contained 1 to 5 percent orthopyroxene of composition $En_{90}$, which has an $SiO_2/MgO$ ratio of 1.65. The data suggest that serpentinization of the Red Mountain-Del Puerto ultramafic rocks proceeded with minimal chemical changes, and therefore imply an appreciable volume increase of the serpentinized parts of the rocks.

## REFERENCES

Bailey, E. H., Irwin, W. P., and Jones, D. L., 1964, Franciscan and related rocks, and their significance in the geology of western California: California Div. Mines and Geology Bull. 183, 177 p.

Barnes, Ivan, LaMarche, V. C., Jr., and Himmelberg, G. R., 1967, Geochemical evidence of present-day serpentinization: Science, v. 156, p. 830–832.

Bodenlos, A. J., 1950, Geology of the Red Mountain magnesite district, Santa Clara and Stanislaus Counties, California: California Jour. Mines and Geology, v. 46, p. 223–278.

Challis, G. A., 1965, The origin of New Zealand ultramafic intrusions: Jour. Petrology, v. 6, p. 322—364.

Duncumb, Peter, and Shields, P. K., 1966, Effect of critical excitation potential on the absorption correction, *in* McKinley, T. D., Henrich, K. F. J., and Witttry, D. B., eds., The electron microprobe. Proceedings of the symposium sponsored by the Electrothermic and Metallurgy Division, the Electrochemical Society, Washington, D.C., 1964: New York, John Wiley and Sons, p. 284–295.

Green, D. H., 1964, The petrogenesis of the high-temperature peridotite instrusion in the Lizard area, Cornwell: Jour. Petrology, v. 5, p. 134–188.

Hawkes, H. E., Jr., Wells, F. G., and Wheeler, D. P., Jr., 1942, Chromite and quicksilver deposits of the Del Puerto area, Stanislaus County, California: U.S. Geol. Survey Bull. 936–D, p. 79–110.

Heinrich, K. F. J., 1966, X-ray absorption uncertainty, *in* McKinley, T. D., Heinrich, K. F. J., and Wittry, D. B., eds., The electron microprobe, Proceedings of the symposium sponsored by The Electrothermic and Metallurgy Division, The Electrochemical Society, Washington, D.C., 1964: New York, John Wiley and Sons, p. 396–377.

Hostetler, P. B., Coleman, R. G., Mumpton, F. A., and Evans, B. W., 1966, Brucite in alpine serpentinites: Am. Mineralogist, v. 51, p. 75–98.

Howie, R. A., and Smith J. V., 1966, X-ray emission microanalysis of rock-forming minerals; V, Orthopyroxenes: Jour. Geology, v. 74, p. 443–462.

Irvine, T. N., 1967, Chromian spinel as a petrogenetic indicator; Pt. 2, Petrologic applications: Canadian Jour. Earth Sci., v. 4, p. 71–103.

Jackson, E. D., 1961, Primary textures and mineral associations in the ultramafic zone of the Stillwater Complex, Montana: U.S. Geol Survey Prof. Paper 358, 106 p.

Jackson, E. D., Stevens, R. E., and Bowen, R. W., 1967, A computer-based procedure for deriving mineral formulas from mineral analyses, *in* Geological Survey Research 1967: U.S. Geol. Survey Prof. Paper 575–C, p. C23–C31.

Maddock, M. E., 1964, Geologic map and sections of the Mount Boardman quadrangle, Santa Clara and Stanislaus Counties, California: California Div. Mines and Geology Map Sheet 3, scale about 1 inch to 1 mile.

Page, N. J., 1967, Serpentinization at Burro Mountain, California: Contr. Mineralogy and Petrology, v. 14, p. 321–342.

Philibert, J., 1963, A method for calculating the absorption correction in electron probe microanalysis, *in* Pattee, H. H., Cosslett, V. E., and Engström, A., eds., X-ray optics and X-ray microanalysis, Proceedings of the Third International Symposium on X-ray optics and X-ray microanalysis, Stanford, 1962: New York, Academic Press, p. 379–392.

Rogers, T. H., 1966, Geologic map of California, Olaf P. Jenkins edition—San Jose sheet [San Francisco, Calif.]: California Div. Mines and Geology, scale 1: 250,000.

Ross, C. S., Foster, M. D., and Myers A. T., 1954, Origin of dunites and of olivine-rich inclusions in basaltic rocks: Am. Mineralogist, v. 39, p. 693–737.

Shapiro, Leonard, and Brannock, W. W., 1962, Rapid analysis of silicate, carbonate, and phosphate rocks: U.S. Geol. Survey Bull. 1144–A, 56 p.

Soliman, S. M., 1965, Geology of the east half of the Mount Hamilton quadrangle, California: California Div. Mines and Geology Bull. 185, 32 p.